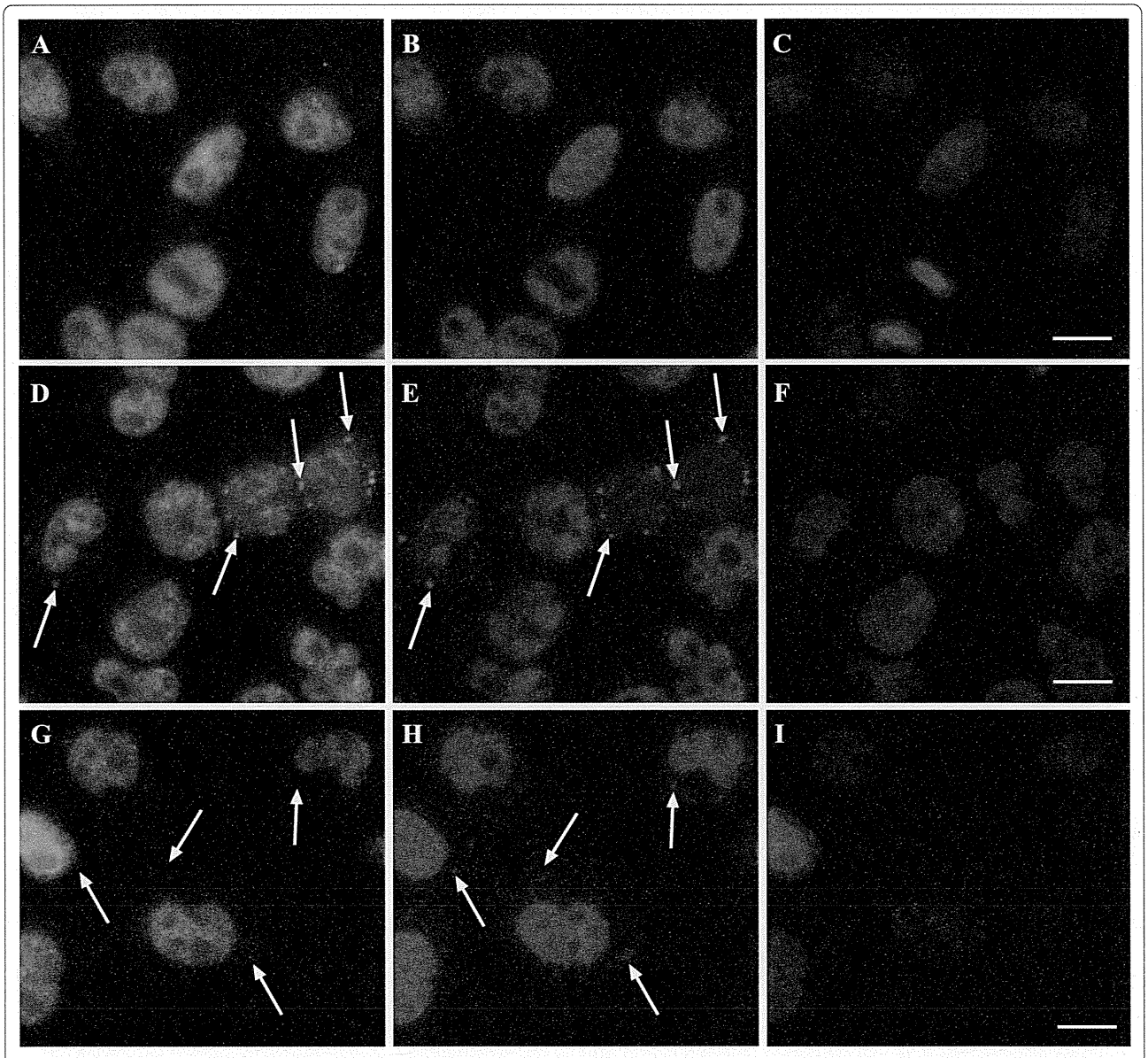

Figure 8 Treatment of HeLa cells with sodium arsenite induces JNK-dependent TDP-43 SGs. HeLa cells were treated for 1 hr with 0.5 mM sodium arsenite and cells were examined for TDP-43 and HuR localization by immunofluorescence. **A-C**: untreated, **D-F**: sodium arsenite-treated, **G-I**: sodium arsenite and SP600125. Green = TDP-43, red = HuR, blue = DAPI. Arrows indicate SGs. Bar = 10 μm. Representative images from three separate experiments performed in duplicate or triplicate.

[25,42] and that stress kinases including JNK can control the cellular localization and SG association of these hnRNPs [31-36]. Analysis of TDP-43 and hnRNP A1 during paraquat stress did not reveal any co-localization within SGs (Figure 10N-Q). In contrast, paraquat-treated cells revealed significant co-localization of hnRNP K and TDP-43 in SGs (Figure 10F-I). Interestingly, JNK inhibition fully blocked both TDP-43 and hnRNP K SG accumulation (Figure 10J-M). As hnRNP K is known to bind to TDP-43, associate with SGs and is phosphorylated by JNK, these findings suggest that modulation of TDP-43 SG association by JNK could be controlled through binding to hnRNP K. However, a comprehensive analysis of hnRNP interactions with JNK and TDP-43 is required to determine if this is the mechanism occurring in paraquat-treated cells and other stress-associated conditions leading to TDP-43 accumulation.

Discussion

Despite considerable research into TDP-43 in the past five years, little is known about the earliest pathological events associated with TDP-43 accumulation in ALS

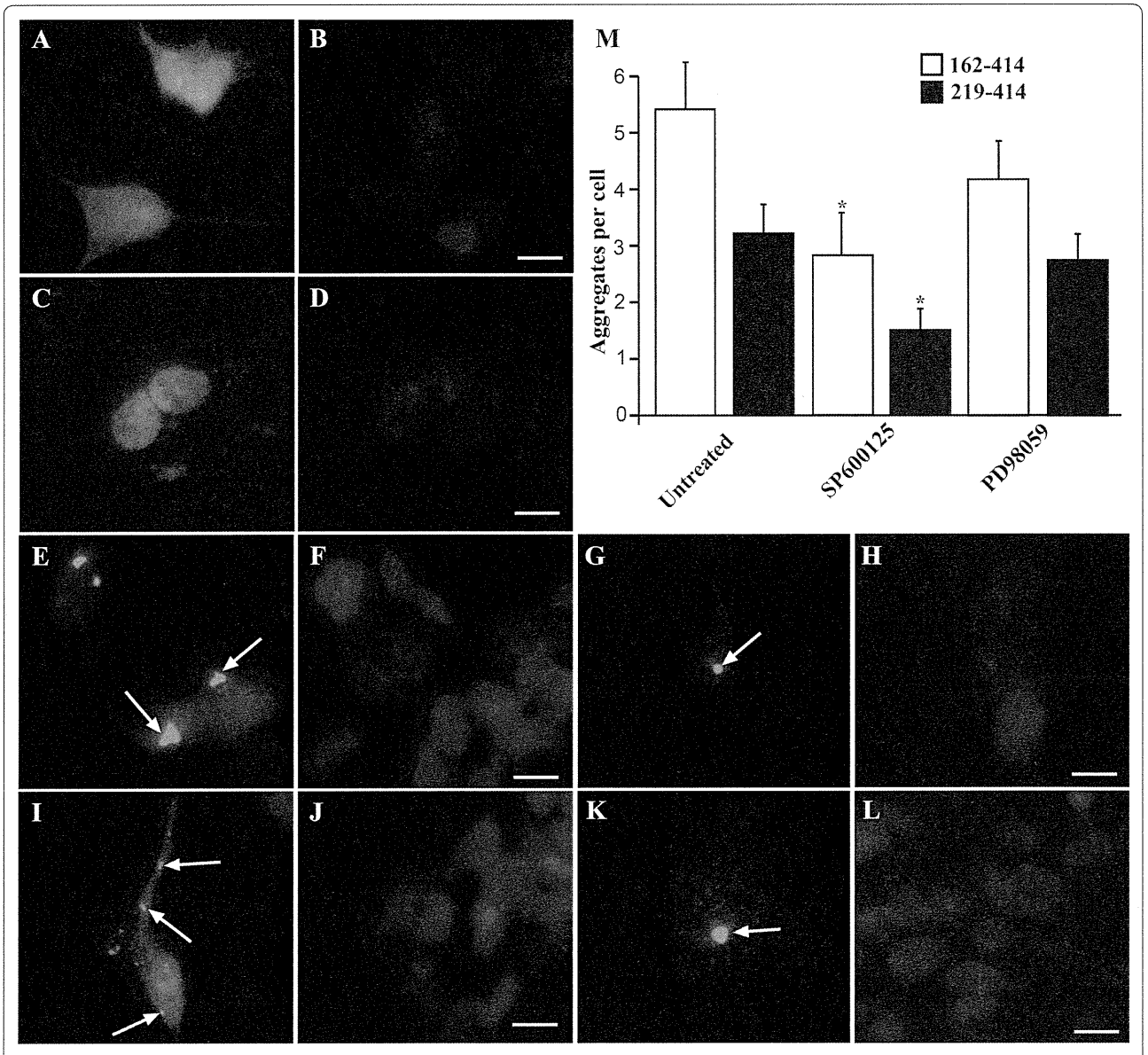

Figure 9 Aggregation of CTF-TDP-43 162-414 and 219-414 in SY5Y cells is partially associated with JNK. SH-SY5Y cells were transfected with GFP-tagged constructs for vector control (**A-B**), full length TDP-43 (**C-D**), CTF-TDP-43 219-414 (**E-H**) or CTF-TDP-43 162-414 (**I-L**). Green = TDP-43-GFP, blue indicates DAPI. Arrows indicate TDP-43 aggregates. Bar = 10 μm. Cells were transfected with CTF-TDP-43 162-414 or 219-414 for 24 hr and co-treated with SP600125 (JNK inhibitor) (**G-H** and **K-L**) or PD98059 (ERK inhibitor) (not shown) for a further 24 hr. The number of TDP-43-GFP aggregates per cell was determined (**M**). **$p < 0.01$. Representative images from two separate experiments performed in triplicate.

and FTD. In this study, we have developed a model of oxidative stress to investigate changes to endogenous TDP-43 processing during cell stresses that reflect the chronic nature of ALS and FTD. We show here that mild stress induced by paraquat, a well-characterized mitochondrial inhibitor and oxidative stress inducer, induced changes to TDP-43 metabolism that closely recapitulated features observed in brain and/or spinal cord of FTD and ALS patients. These changes included clearance of TDP-43 from cell nuclei, accumulation of diffuse TDP-43 in cytosol, aggregation into SGs, ubiquitination of a portion of these SGs and increased expression of the 35 kDa CTF-TDP-43. These are all considered important hallmarks of TDP-43 proteinopathies [6,8]. Importantly, we also found these changes to TDP-43 metabolism in differentiated neurons and additional cell-lines demonstrating that this was not a cell-specific effect. In addition, short term treatment of cells with paraquat (1 hr) had no effect on TDP-43, providing strong support for chronic cell stress as an important

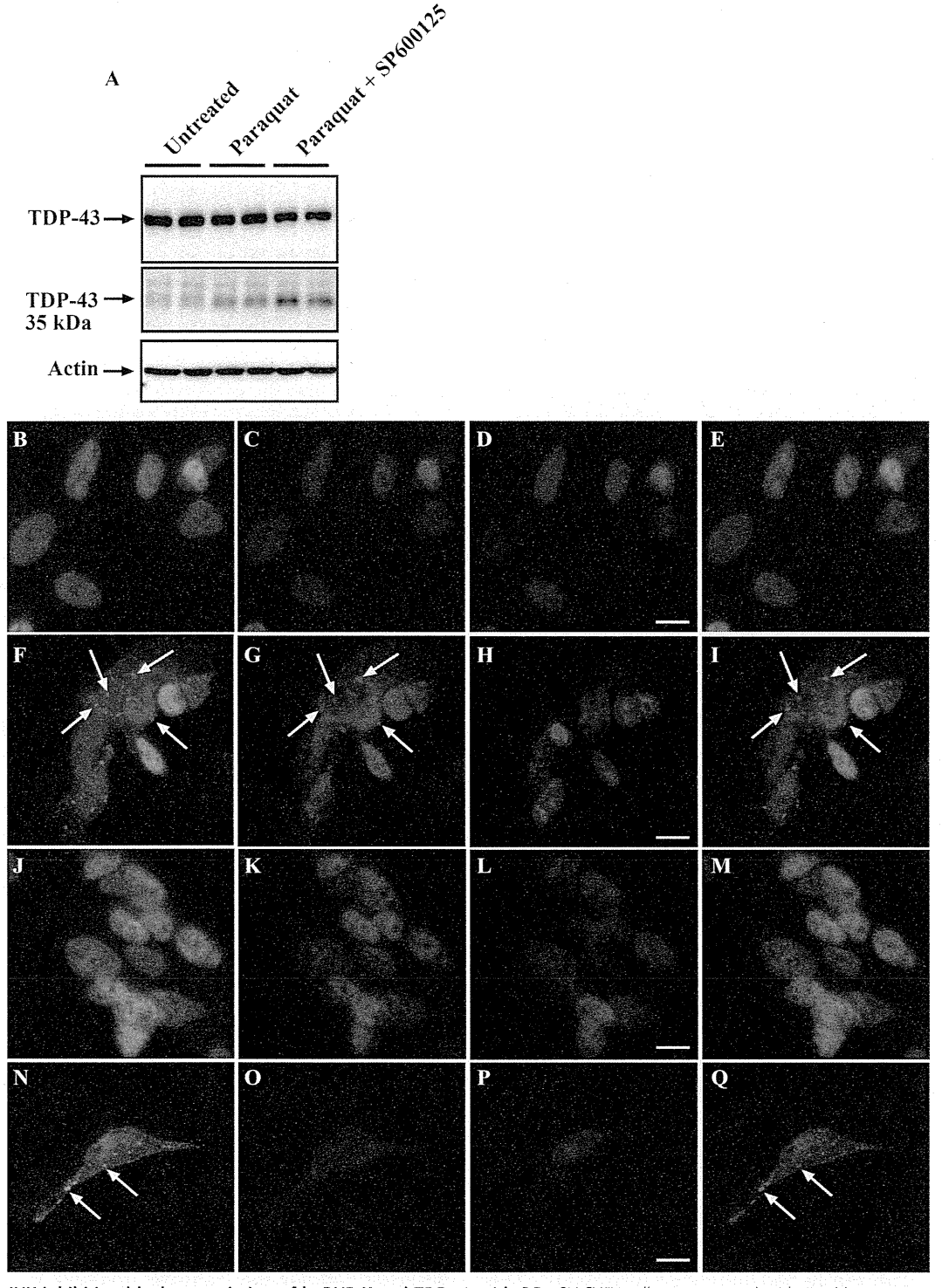

Figure 10 JNK inhibition blocks association of hnRNP K and TDP-43 with SGs. SH-SY5Y cells were treated with 1 mM paraquat overnight in the presence and absence of SP600125. **A**: Cells were immunoblotted for full length TDP-43 and 35 kDa CTF-TDP-43, **B-Q**: Cells were treated with paraquat and SP600125 and examined for TDP-43, hnRNP K or hnRNP A1 by immunofluorescence. **B-E**: untreated, labeled for TDP-43 (green) and hnRNP K (red); **F-I**: paraquat-treated, labeled for TDP-43 (green) and hnRNP K (red); **J-M**: paraquat and SP600125, labeled for TDP-43 (green) and hnRNP K (red); **N-Q** paraquat-treated, labeled for TDP-43 (green) and hnRNP A1 (red). Right-hand panel indicates merged images from TDP-43 and hnRNP panels. Arrows indicate SGs. Bar = 10 μm. Representative images from three separate experiments performed in duplicate or triplicate.

mediator of TDP-43 abnormal processing as observed in ALS and FTD CNS tissues.

The key finding of this study was that cell kinase activity and in particular, JNK activation, modulates TDP-43 localization to SGs. This is the first report of TDP-43 localization controlled by kinase activity. This process is perhaps not surprising as previous reports describe the nuclear-cytoplasmic movement and SG localization of alternative hnRNPs and HuR. Habelhah et. al., have shown that phosphorylation of hnRNP K by ERK can modulate cytoplasmic accumulation [34]. In a separate study they also demonstrated that hnRNP K is phosphorylated by JNK at serine 216 and serine 353 [43]. Moreover, p38 phosphorylates hnRNP A1 inducing SG localization [35,36]. There is also evidence that JNK modulates localization and activity of HuR [44]. Importantly, several studies have shown that HuR and hnRNP A1 and K as well as other hnRNPs directly bind TDP-43 [25,42,45]. Interestingly this is mediated through interaction at the C-terminal region of both proteins. The C-terminal domain of TDP-43 is where the majority of known ALS/FTD disease mutations have been identified [11]. Moreover, there are key JNK phosphorylation consensus sites (Ser/Thr-Pro) within the C-terminal region of hnRNP K and HuR [43]. It is possible that kinase (especially JNK) phosphorylation of hnRNPs modulates interaction with TDP-43, thus mediating SG association. Alternatively, specific phosphorylation of hnRNPs may simply target them to SGs and due to TDP-43 association with these hnRNPs, it becomes localized to SGs where hnRNPs are present. Further support for an hnRNP-TDP-43 association was found in our model where we showed that JNK inhibition blocked localization of both TDP-43 and hnRNP K to SGs. This is particularly interesting as hnRNP K is phosphorylated by JNK [43] and the phosphorylation site lies within the hnRNP C-terminal domain that interacts with TDP-43 in studies on other hnRNPs [42]. Further support for this was shown by the fact that there was no specific localization of hnRNP A1 with paraquat-induced TDP-43 SGs in our study. Interestingly, the only JNK phosphorylation consensus site on hnRNP A1 is in the N-terminal region (Ser7/Pro8) rather than in the C-terminal region that would interact with TDP-43. In addition to these findings, we observed that JNK inhibition did not decrease CTF-TDP-43 generated by paraquat treatment and in fact increased expression. This indicated that JNK is more likely to be controlling localization of cytoplasmic TDP-43 to SGs similar to that reported for other kinases and hnRNPs, rather than modulating the formation of CTF-TDP-43. Whether it is CTF-TDP-43 or full length TDP-43 or both that is aggregating into SGs in this model remains to be seen. Due to the loss of nuclear TDP-43 expression and the fact that CTF-TDP-43 only accounted for approximately 10% of total TDP-43 on Western blots, strongly suggested that the SGs probably contained full length TDP-43 or a mixture of full length and CTF-TDP-43.

There must also be additional factors associated with TDP-43 localization to SGs. JNK activation is not specific for paraquat and in fact, alternative mitochondrial inhibitors used in this study also induce JNK activation [38]. Phosphorylation of JNK is a common downstream effect of oxidative and other cells stresses. The specificity of paraquat to induce JNK-mediated localization of TDP-43 may be related to specific sub-cellular localization of activated JNK or modulation of additional co-factors. Considerable investigation will be required to delineate the specific processes induced by paraquat that leads to JNK-mediated TDP-43 SG accumulation and how these may relate to neurodegenerative diseases such as ALS.

While some recent studies have reported a possible association between TDP-43 and TIA-1 [16,17], these have been demonstrated with transfected cells and no clear evidence of endogenous TDP-43-TIA-1 interaction was identified. Moreover, TIA-1 does not contain JNK consensus sites and there are no reports of JNK control of TIA-1 localization. We believe that the data presented here are more consistent with a potential interaction between TDP-43 and hnRNP K (Figure 11). However, further studies will be required to demonstrate specific interaction in this chronic stress model and to determine if mutation of the C-terminal JNK phosphorylation site on hnRNP K prevents TDP-43 association with SGs. It was also clear from our findings that additional kinases can control TDP-43 and probably a range of hnRNPs during stress. It will take a considerable effort to delineate the role of p38, ERK and additional kinases on TDP-43 accumulation both *in vitro* and *in vivo*.

We also observed partial JNK-mediated control of TDP-43 localization to SGs induced by sodium arsenite, the most common method used for SG induction. The lack of complete inhibition of TDP-43 SG accumulation was possibly related to the fact that sodium arsenite rapidly induces SGs (minutes), while paraquat had no effect on TDP-43 in short-term treatment even at very high doses. This suggests that while sodium arsenite and paraquat induce SGs and both involve JNK, there are different cellular mechanisms involved in short term and longer term SG formation. This is consistent with the previously reported concept that different stresses have diverse affects on SG formation [18]. In this context, we feel that our paraquat-based mild oxidative stress model is an important tool for delineating TDP-43 SG association as it occurs under mild stress conditions expected in chronic neurodegenerative diseases

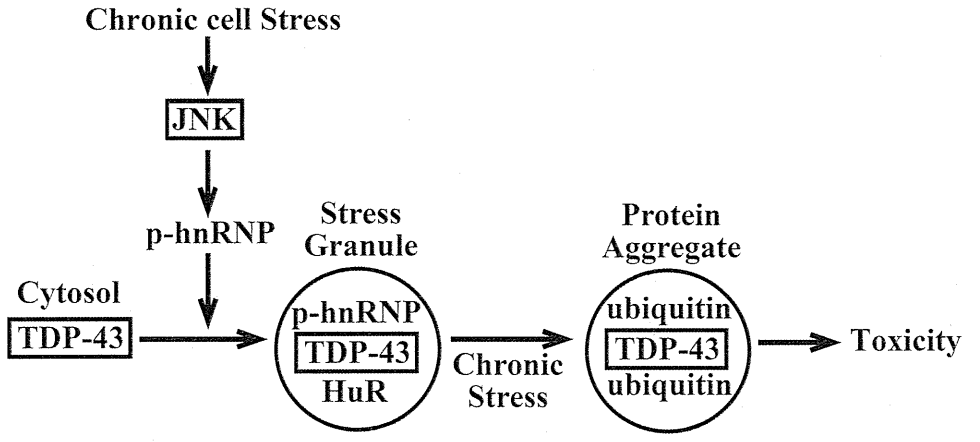

Figure 11 Schematic of proposed stress-mediated TDP-43 accumulation into SGs. Chronic cell stress (eg oxidative stress) induces activation of stress kinases such as JNK. This may phosphorylate hnRNPs such as hnRNP K resulting in phosphoryated forms (p-hnRNP). This could modulate interaction with TDP-43 and association with SGs. Prolonged stress may lead to progression of SGs to protein aggregates containing TDP-43 and subsequent cell toxicity.

and better re-capitulates the features of TDP-43 proteinopatheis than sodium arsenite. It is possible that the latter, (ie acute sodium arsenite exposure) rapidly drives SG formation in cells that are experiencing high levels of toxicity. As shown in Additional File 1B, treatment with 500 μM sodium arsenite overnight results in almost total loss of cell viability as compared to only 15% decrease in viability with 1 mM paraquat overnight.

Whether JNK directly modulates TDP-43 is not known. TDP-43 does not contain known consensus sites for JNK, p38 or ERK. However, it does contain two putative JNK binding domains (RxxxKxxxLxV and KxxRxxxxVxF) at 98-108 and 224-235 respectively. It remains a possibility that JNK binds to TDP-43 and acts as a scaffolding protein affecting SG localization. While no other studies have demonstrated a TDP-43-JNK association, a previous report described a role for a JNK-interacting protein, WDR62 in SG formation [41]. Interestingly, they reported that inhibition of JNK during sodium arsenite treatment increased the number of SGs (in HEK293 cells) but decreased the size of the granules. This is in contrast to our finding in HeLa cells where we found a partial decrease in TDP-43 SG association but no observable changes to HuR SG formation with SP600125. In addition, JNK inhibition did not block SG formation by paraquat as determined by HuR staining but did block TDP-43 and hnRNP K localization. However, these differences are again likely to be due to acute sodium arsenite treatment compared to longer paraquat treatment used here, different cell lines and different markers of SGs eg HuR and TIA-1. Importantly, the findings show that different model systems may give a range of different outcomes and in terms of understanding TDP-43 pathological changes, it will be important to ensure that the model gives an accurate reflection of the disease processes. With that in mind, we are currently investigating TDP-43 metabolism in primary neuronal and glia cell cultures as this may be a more accurate model system to understand TDP-43 SG dynamics.

The role for stress kinases such as JNK and p38 in ALS has been suggested through recent studies. SOD1 ALS models have shown enhanced activity of these kinases as well as modulation of ERK [46-50]. Interestingly, a recent report by Ayala et al. [51] found ERK aggregates in stressed cells and ALS tissues and inhibition of ERK lead to increased TDP-43 aggregation in cultures. While these affects appear to contrast with our own findings, the differences may reflect different intensity and form of stress as well as different cell models and time frame. It will be important to determine the kinetics of ERK and other kinases activation across the disease course in ALS. A single report on JNK activation in ALS patients has described increased activity in astrocytes but not neurons in spinal cord of these patients [52]. We found that paraquat induced TDP-43 aggregation in both neuronal-like and astroglial cell lines in this study. Whether JNK or additional kinases are associated with early changes to TDP-43 accumulation in vivo is not known due to the difficulty of obtaining relevant early disease tissues. It is likely that with the current development of multiple animal models of TDP-43 proteinopathy that re-capitulate human disease neuropathology, we will be able to determine the early events in TDP-43 processing. It is also uncertain what role hnRNPs have in determining TDP-43 aggregation in ALS or FTD. While a large number of hnRNPs have been shown to bind to TDP-43 and many are associated

with SGs, their role in ALS and FTD has not been established. It is important to note, however, that several recent studies have shown that TDP-43 and FUS are associated with SG marker proteins in ALS tissues [17,24].

An important outcome from this study is that kinases may be an important target for therapeutic intervention in ALS and FTD. Should further studies show that kinase activation controls TDP-43 aggregation especially early in disease, it may be possible to inhibit this process with kinase inhibitors. Interestingly, the only approved treatment for slowing ALS disease progression, Riluzole, is known to modulate stress kinase activity [53], and kinase modulators have been discussed previously as possible therapeutic agents for ALS.

Conclusions

In summary, it has been difficult to accurately model endogenous aberrant TDP-43 in cell models. Treatment of cells with sodium arsenite or osmotic stress induces robust TDP-43 containing SGs however, these models have not recapitulated the broad features of TDP-43 mis-metabolism observed in ALS and FTD brain and spinal cord tissues in a manner consistent with transfection of CTF-TDP-43 constructs. The latter however, are likely to be prone to spontaneous aggregation when over-expressed and may not represent an accurate model of the cellular control of TDP-43 processing during chronic stress. Likewise, although studies with mutant TDP-43 constructs can help to understand the disease processes, the majority of ALS and FTD cases are sporadic and probably involve only endogenous, non-mutated TDP-43. Our model has recapitulated a number of features of aberrant endogenous TDP-43 metabolism including loss of nuclear staining, accumulation of diffuse cytoplasmic TDP-43, formation of CTF-TDP-43, aggregation into SGs and ubiqitination of a portion of these SGs indicating the possible transition to irreversible protein aggregates. The aggregation of TDP-43 into SGs is controlled by JNK and SG formation is controlled by additional kinases and these factors are associated with chronic stress. Future studies will be required to fully delineate the mechanism by which kinases control TDP-43 aggregation and whether this is involved in TDP-43 aggregation in vivo. These findings may have important implications for identifying potential therapeutic targets for intervention in ALS and FTD.

Methods

Materials

4',6' Diamino-2-phenylindole dihydrochloride (DAPI) was obtained from Invitrogen (Mount Waverley, Victoria, Australia). (3-(4,5-Dimethylthiazol-2-yl)-2,5-diphenyltetrazolium bromide (MTT), N, N'-dimethyl-4,4'-bipyridinium dichloride (paraquat), rotenone, 1-methyl-4-phenylpyridinium (MPP+), sodium azide, sodium arsenite, 3-nitropropionic acid (3-NP) and 3-Morpholinosyndnomine (SIN-1) were from Sigma Aldrich (Sydney, NSW, Australia) and LDH assay kit was purchased from Roche Diagnostics (Castle Hill, NSW, Australia). SP600125, PD98095, SB203580 were purchased from Merck Biosciences (Melbourne, Victoria, Australia). BI-78D3 and D4476 were purchased from Tocris Bioscience (Ellisville, Melbourne, Victoria, Australia). Z-VAD-fmk was obtained from Promega (Sydney, Australia).

Polyclonal TDP-43 antisera were purchased from Proteintech Group (Chicago, IL, USA). Monoclonal antisera to the phosphorylated form of TDP-43 (ser409/410) were obtained from Cosmo Bio (Tokyo, Japan). Antisera to ubiquitin were from Santa Cruz Biotechnology (Santa Cruz, CA, USA). Monoclonal antisera to hnRNP A1 and hnRNP K were purchased from Abcam (Waterloo, Australia). Monoclonal antisera to HuR were obtained from Invitrogen (Mount Waverley, Victoria, Australia). Antisera to total and phosphorylated forms of p38, ERK and JNK, as well as antibodies to actin and GAPDH were purchased from Cell Signalling Technologies (Arundel, Queensland) or BD Bioscience (North Ryde NSW, Australia).

Methods

Cell Culture

The cell lines used in this study were human neuroblastoma SH-(SY5Y) cell line, human epithelial HeLa cell line, human embryonic kidney cell line (HEK293), human fibroblast cell line (GSM2069) and human astroglial U87MG cell line. Cells were passaged and maintained in DMEM plus 5% FBS (HeLa and HEK293 cells), DMEM/F12 plus 10% FBS (SH-SY5Y and U87MG cells) or BME plus 10% FCS (GSM2069 fibroblasts). To induce differentiation, SY5Y cells were treated with 10 μM retinoic acid for 7 days. Differentiation was confirmed by morphological changes (neurite extension) and up-regulated expression of synaptophysin, tyrosine hydroxylase and VMAT2. All cells were grown in 5% CO_2 at 37°C.

Cell viability and cell lysis assays

Assays for cell viability (MTT) and cell lysis (LDH) were performed as previously described [28].

Exposure of cell to stress

Undifferentiated cells were grown in 24 or 6-well plates or on 12 mm coverslips (for immunofluorescence) for 2-3 days before experiments (~80% confluent). Differentiated SH-SY5Y cells were cultured in the presence of retinoic acid for 7 days before experiments. Inducers of

nitrosative stess (arginine, paraquat and SIN-1) or oxidative stress (rotenone, 3-NP, sodium azide, MPP+, sodium arsenite and paraquat) were prepared in dH_2O and added at indicated concentrations and the medium was briefly mixed by aspiration. Incubations were performed for periods stated in individual experiments. Where indicated, cells were co-treated with kinase inhibitors (SP600125 (JNK), BI-78D3 (JNK), PD98095 & U0126 (ERK), SB203580 & SB202190 (p38), D4476 (casein kinase 1) from stock solutions prepared at 10 mM in DMSO. Control cultures were treated with vehicle alone. For immunoblotting, cells were harvested into Phosphosafe Extraction Buffer (Merck Biosciences, San Diego, CA, USA) containing protease inhibitor cocktail (Roche Diagnostics) and stored at -80°C until use. For immunofluorescence studies, cells were grown on glass coverslips and fixed by treating with 4% paraformaldehyde for 30 min.

siRNA knockdown of JNK

ON-TARGETPlus human JNK1 siRNA pool, JNK2 siRNA pool and non-targeting siRNA pool (D-001810-10-20, Negative control) were obtained from Dharmacon and resuspended in RNAase free water at 100 μM. Human JNK1 siRNA pool target sequences were 5'-GCCCAGUAAUAUAGUAGUA-3', 5'-GGCAUGGGCUACAAGGAAA-3', 5'-GAAUAGUAUGCGCAGCUUA-3' and 5'-GAUGACGCCUUAUGUAGUG-3'. Human JNK2 siRNA pool target sequences were 5'-UCGUGAACUUGUCCUCUUA-3', 5'-AGCCAACUGUGAGGAAUUA-3', 5'-GGCUGUCGAUGAUAGGUUA-3' and 5'-GAUUGUUUGUGCUGCAUUU-3'. Cells were seeded on coverslips at 5×10^4 cells per cm^2 in Opti-MeM to give 40% confluency on treatment day. Cells were transfected with pooled JNK1 and JNK2 siRNA or Negative control siRNA in Lipfectamine 2000 for 5 hr at room temperature (0.5 μg RNA per well). Media was then replaced with normal SY5Y growth medium overnight before treatment with paraquat (1 mM) overnight. Cells were then collected for Western blot for JNK or fixed for immunofluoresence of TDP-43 and HuR.

Western blot analysis of protein expression and phosphorylation

Cell lysates prepared in Phosphosafe Extraction Buffer at equal protein concentration were mixed with electrophoresis SDS sample buffer and separated on 12% SDS-PAGE Tris-Glycine gels. Proteins were transferred to PVDF membranes and blocked with 4% skim milk solution in PBST before immunoblotting for total or phospho-specific proteins. For detection of total TDP-43, membranes were probed with polyclonal antisera (1:1500) against TDP-43. Secondary antiserum was rabbit-HRP at 1:5,000 dilution. For detection of total and phospho-forms of JNK, ERK and p38, membranes were probed with anti-JNK, anti-ERK or anti-p38 (each at 1:5000) and antisera to phospho-forms of each protein (each at 1:5000). Blots were developed using GE Healthcare ECL Advance Chemiluminescence and imaged on a Fujifilm LAS3000 imager (Berthold, Bundoora, Australia). Expression of GAPDH or actin was determined using antisera at 1:5000 and 1:3000 respectively for protein loading controls where necessary.

Immunofluorescence analysis

SH-SY5Y cells were grown on 12 mm diameter coverslips and treated with stresses as indicated. Cells were fixed with 4% w/v paraformaldehyde in PBS for 30 min and permeabilized with 90% chilled methanol for 5 min. After blocking for 1 hr with 10% normal goat serum, cells were incubated with primary antibody for total TDP-43 (1:1500), ubiquitin (1:150), HuR (1:50), hnRNP A1 (1:200) or hnRNP K (1:200) for 2 hr at room temperature or overnight at 4°C. This was followed by labeling with secondary AlexaFluor or FITC goat anti-mouse or anti-rabbit antisera at 1:500 for 2 hr at room temperature or overnight at 4°C. After washing, the coverslips were incubated with DAPI at 0.5 μg/ml for 5 min and analyzed using a Leica inverted microscope with Zeiss Axiocam digital camera. Images shown are representative of multiple fields and triplicate coverslips per experiment. TDP-43 and HuR-positive stress granules (SGs) were counted in cultures where indicated. A minimum of 500 cells was counted across multiple fields of view (and multiple coverslips) for each treatment. The number of TDP-43 and HuR-positive SGs were counted in these cells. The total number of cells was divided by the total number of SGs to provide a measure of mean SGs per cell. SGs were not observed in untreated cells.

Preparation of TDP-43 plasmids

Plasmid DNA corresponding to GFP-tagged full-length wild-type (WT) TDP-43 (pEGFP-TDP WT), C-terminal fragments of TDP-43, (pEGFP-TDP 162-414 and pEGFP-TDP 219-414) or empty expression vector pEGFP-C1 were prepared as described by Nonaka et al. [15]. Briefly, plasmid DNA was used to transform MAX Efficiency® DH5α™ Competent Cells (Invitrogen, Mount Waverley, Victoria, Australia) as described by the manufacturer. Transformants were grown and colonies were picked based on kanamycin-resistance and grown in liquid culture for subsequent plasmid purification. DNA was purified using the Wizard® *Plus* Midiprep DNA Purification System (Promega Corporation) as per manufacturer's instructions. DNA was quantified and TDP-43 inserts were identified positively by digestion with *BamHI* and *XhoI*.

Transfection and expression of plasmids

SH-SY5Y cells were seeded at 2 × 10^5 cells per well in 24 well-plates on coverslips. Cells were transfected 24 hr after seeding with the pEGFP-C1 empty vector, pEGFP-TDP WT, pEGFP-TDP 162-414 and pEGFP-TDP 219-414 using Attractene (Qiagen) according to manufacturer's instructions. After 48 hr incubation, cells were fixed with 4% w/v paraformaldehyde in PBS for 30 min. and permeabilized with 90% chilled methanol for 5 min. After washing, the coverslips were incubated with DAPI at 0.5 μg/ml for 5 min and analyzed using a Leica inverted microscope with Zeiss Axiocam digital camera. Expression of TDP-43 was determined by the EGFP-tagged construct. Efficiency of transfection with pEGFP-C1 vector was approximately 20-25%.

Statistical analysis

All data described in graphical representations are mean ± standard error of the mean (SEM) unless stated from a minimum of three experiments. Results were analysed using a two-tailed Student's *t*-test.

Additional material

Additional file 1: SH-SY5Y cell viability after exposure to nitrosative or oxidative stress inducers. SH-SY5Y cells were treated with indicated compounds overnight and cell viability was measured with the MTT assay. **A:** Mild neurotoxicity was induced with all compounds tested. Concentrations were SIN-1, 0.1 mM; arginine, 1 mM; Paraquat, 1 mM and 2 mM; 3-NP, 1 mM; MPP+, 2 mM; sodium azide, 5 mM and rotenone, 0.075 mM. **B:** Comparison of neurotoxicity induced by 1 and 2 mM paraquat or 0.05 mM and 0.5 mM arsenite treatment overnight. *p < 0.05, **p < 0.01. n = three experiments.

Additional file 2: Treatment of SH-SY5Y neurons induces SG formation associated with mild toxicity. Non-differentiated (**A-C**) or differentiated (**D-K**) were treated with 0-2 mM (**A-C**) or 1 mM (**D-K**) paraquat overnight. **A**: Cell viability was determined by MTT assay. **B**: Cell death was determined by LDH assay. **C**: Stress granules (SGs) per cell were determined. *p < 0.05, **p < 0.01. **D-K**: TDP-43 and HuR immunofluorescence was examined in retinoic acid-differentiated neurons after treatment with 1 mM paraquat. Green = TDP-43, Red = HuR, Blue = DAPI. Arrows indicate SGs. Bar = 10 μm. **G** and **K** represent merged images. n = three experiments.

Additional file 3: Paraquat treatment did not induce phosphorylation of TDP-43 in SGs. Cells were treated overnight with 1 mM paraquat and examined for phosphorylated TDP-43 by immunofluorescence. **A-C:** untreated, **D-F:** paraquat treated. Green = HuR, Red = phospho-TDP-43, blue = DAPI. Bar = 10 μm. **G:** Immunoblot for phospho-TDP-43 (p-TDP-43) in paraquat-treated cultures. Representative images from three separate experiments.

Additional file 4: Treatment of SH-SY5Y cells with different mitochondrial inhibitors did not induce HuR SGs. Cells were treated with vehicle control (**A-B**), 2 mM MPP+ (**C-D**), 1 mM 3-NP (**E-F**), 0.075 mM rotenone (**G-H**) or 5 mM sodium azide (**I-J**). Cells were analyzed for HuR localization by immunofluorescence. Red = HuR, blue = DAPI. Bar = 10 μm. **K:** Treatment with 1 mM paraquat (PQ) overnight induced phospho-JNK (pJNK) and this was inhibited by co-treatment with 20 μM SP600125. Representative images from three separate experiments.

Additional file 5: Treatment of SH-SY5Y cells with siRNA to JNK inhibits TDP-43 accumulation in SGs. A: Cells were treated with pooled siRNA against JNK1 and JNK2 or with negative control siRNA and examined for JNK expression. siRNA to JNK significantly reduced expression of JNK1 and JNK2. **B-E:** Untreated control cells. **F-I:** cells treated with negative control siRNA reveal TDP-43 and HuR-positive SGs. **J-M:** Cells treated with siRNA to JNK reveal lack of TDP-43 but not HuR-positive SGs. Green = TDP-43, red = HuR, blue - DAPI. Arrows indicate SGs. Bar = 10 μm. Representative images from two-three separate experiments performed in triplicate.

Additional file 6: Treatment of U87MG astroglial and HeLa epithelial cells with paraquat results in TDP-43 SGs. U87MG (**A-F**) and HeLa (**G-L**) cells were treated overnight with 1 mM paraquat and analyzed for TDP-43 and HuR localization by immunofluorescence. **A-C**: Untreated U87MG cells, **D-F**: paraquat-treated U87MG cells, **G-I**: untreated HeLa cells, **J-L**: paraquat-treated HeLa cells. Green = TDP-43, red = HuR, blue = DAPI. Arrows indicate SGs. Bar = 10 μm. Representative images from three separate experiments performed in duplicate or triplicate.

Abbreviations

ALS: amyotrophic lateral sclerosis; CTF: C-terminal fragment; ERK: extracellular signal-regulated kinase; FTD: frontotemporal dementia; hnRNP: heterogeneous nuclear ribonucleoprotein; JNK: c-JUN N-terminal kinase; SG: stress granule; SOD: superoxide dismutase; TDP-43: TARDP-binding protein 43.

Acknowledgements

This work was supported by funding from the National Health and Medical Research Council of Australia (program grant to ARW and CLM) and the Australian Research Council of Australia (ARC Future Fellowship to Anthony White). Dominic Ng is a recipient of a Faculty of Medicine, Dentistry and Health Sciences, CR Roper Fellowship. Peter Crouch is recipient of a Melbourne Neuroscience Institute Research Fellowship. We would also like to thank the Motor Neuron Disease Research Institute of Australia (Mick Rodger Benalla Research Grant), the Bethlehem Griffiths Research Foundation and the CASS Foundation for their kind support of this work. JM was supported by Motor Neuron Disease Research Institute of Australia (Mick Rodger Benalla Research Grant). SJP was supported by the CASS foundation. LJV was supported by the NHMRC. KAP was supported by The University of Melbourne. JRL, AC, Q-XL and PJC were supported by the NHMRC. KMK was supported by Sigrid Juselius Foundation, Finland. CLM was supported by the Mental Health Research Institute. TN and HM were supported by the Tokyo Institute of Psychiatry.

Author details

[1]Department of Pathology, The University of Melbourne, Victoria, 3010, Australia. [2]Ludwig Institute for Cancer Research, Austin Hospital, Harold Stokes Building, 145-163 Studley Road, Heidelberg, Victoria, 3084, Australia. [3]Bio21 Molecular Science and Biotechnology Institute, The University of Melbourne, Parkville, Victoria, 3052, Australia. [4]Department of Biochemistry and Molecular Biology, The University of Melbourne, Parkville, Victoria, 3052, Australia. [5]The Mental Health Research Institute, Parkville, Victoria, 3052, Australia. [6]Department of Molecular Neurobiology, Tokyo Institute of Psychiatry, Tokyo 156-8585, Japan.

Authors' contributions

JM performed cell culture assays, immunofluorescence studies, immunoblotting and contributed to the preparation of the manuscript. SJP performed cell culture assays, immunofluorescence studies, immunoblotting transfected cells with constructs and contributed to the preparation of the manuscript. LJV prepared TDP-43 CTF constructs. KAP prepared, treated and collected cell cultures for analysis. JRL participated in the study design and coordination, contributed to experimental data collection and helped to draft the manuscript. AC performed cell culture assays, immunofluorescence studies, immunoblotting and contributed to the preparation of the manuscript, Q-XL participated in the study design and coordination, contributed to experimental data collection and helped to draft the manuscript. CLM helped to draft the manuscript. TN generated TDP-43 constructs. MH generated TDP-43 constructs. KMK participated in the study design and coordination, contributed to experimental data collection and helped to draft the manuscript. DCHN and MAB developed molecular tools

for JNK analysis and contributed to the preparation of the manuscript. PJC participated in the study design and coordination, contributed to experimental data collection and helped to draft the manuscript. ARW conceived the study, participated in the study design and coordination, and helped to draft the manuscript. All authors read and approved the final manuscript.

Competing interests

The authors declare that they have no competing interests.

Received: 15 April 2011 Accepted: 8 August 2011
Published: 8 August 2011

References

1. King AE, Dickson TC, Blizzard CA, Woodhouse A, Foster SS, Chung RS, Vickers JC: **Neuron-glia interactions underlie ALS-like axonal cytoskeletal pathology.** *Neurobiol Aging* 2009, **32**:459-469.
2. Barber SC, Shaw PJ: **Oxidative stress in ALS: key role in motor neuron injury and therapeutic target.** *Free Radic Biol Med* 2010, **48**:629-641.
3. Swarup V, Julien JP: **ALS pathogenesis: Recent insights from genetics and mouse models.** *Prog Neuropsychopharmacol Biol Psychiatry* 2010, **35**:363-369.
4. Barmada SJ, Finkbeiner S: **Pathogenic TARDBP mutations in amyotrophic lateral sclerosis and frontotemporal dementia: disease-associated pathways.** *Rev Neurosci* 2010, **21**:251-272.
5. Ferrari R, Kapogiannis D, Huey ED, Momeni P: **FTD and ALS: A Tale of Two Diseases.** *Curr Alzheimer Res* 2011, **8**:273-294.
6. Neumann M, Sampathu DM, Kwong LK, Truax AC, Micsenyi MC, Chou TT, Bruce J, Schuck T, Grossman M, Clark CM, McCluskey LF, Miller BL, Masliah E, Mackenzie IR, Feldman H, Feiden W, Kretzschmar HA, Trojanowski JQ, Lee VM: **Ubiquitinated TDP-43 in frontotemporal lobar degeneration and amyotrophic lateral sclerosis.** *Science* 2006, **314**:130-133.
7. Arai T, Hasegawa M, Akiyama H, Ikeda K, Nonaka T, Mori H, Mann D, Tsuchiya K, Yoshida M, Hashizume Y, Oda T: **TDP-43 is a component of ubiquitin-positive tau-negative inclusions in frontotemporal lobar degeneration and amyotrophic lateral sclerosis.** *Biochem Biophys Res Commun* 2006, **351**:602-611.
8. Chen-Plotkin AS, Lee VM, Trojanowski JQ: **TAR DNA-binding protein 43 in neurodegenerative disease.** *Nat Rev Neurol* 2010, **6**:211-220.
9. Banks GT, Kuta A, Isaacs AM, Fisher EM: **TDP-43 is a culprit in human neurodegeneration, and not just an innocent bystander.** *Mamm Genome* 2008, **19**:299-305.
10. Mackenzie IR, Rademakers R, Neumann M: **TDP-43 and FUS in amyotrophic lateral sclerosis and frontotemporal dementia.** *Lancet Neurol* 2010, **9**:995-1007.
11. Warraich ST, Yang S, Nicholson GA, Blair IP: **TDP-43: a DNA and RNA binding protein with roles in neurodegenerative diseases.** *Int J Biochem Cell Biol* 2010, **42**:1606-169.
12. Nishimura AL, Zupunski V, Troakes C, Kathe C, Fratta P, Howell M, Gallo JM, Hortobagyi T, Shaw CE, Rogelj B: **Nuclear import impairment causes cytoplasmic trans-activation response DNA-binding protein accumulation and is associated with frontotemporal lobar degeneration.** *Brain* 2010, **133**:1763-1771.
13. Igaz LM, Kwong LK, Chen-Plotkin A, Winton MJ, Unger TL, Xu Y, Neumann M, Trojanowski JQ, Lee VM: **Expression of TDP-43 C-terminal Fragments in Vitro Recapitulates Pathological Features of TDP-43 Proteinopathies.** *J Biol Chem* 2009, **284**:8516-24.
14. Zhang YJ, Xu YF, Cook C, Gendron TF, Roettges P, Link CD, Lin WL, Tong J, Castanedes-Casey M, Ash P, Gass J, Rangachari V, Buratti E, Baralle F, Golde TE, Dickson DW, Petrucelli L: **Aberrant cleavage of TDP-43 enhances aggregation and cellular toxicity.** *Proc Natl Acad Sci USA* 2009, **106**:7607-12.
15. Nonaka T, Kametani F, Arai T, Akiyama H, Hasegawa M: **Truncation and pathogenic mutations facilitate the formation of intracellular aggregates of TDP-43.** *Hum Mol Genet* 2009, **18**:3353-3364.
16. McDonald KK, Aulas A, Destroismaisons L, Pickles S, Beleac E, Camu W, Rouleau GA, Vande Velde C: **TAR DNA-binding protein 43 (TDP-43) regulates stress granule dynamics via differential regulation of G3BP and TIA-1.** *Hum Mol Genet* 2011, **20**:1400-1410.
17. Liu-Yesucevitz L, Bilgutay A, Zhang YJ, Vanderwyde T, Citro A, Mehta T, Zaarur N, McKee A, Bowser R, Sherman M, Petrucelli L, Wolozin B: **Tar DNA binding protein-43 (TDP-43) associates with stress granules: analysis of cultured cells and pathological brain tissue.** *PLoS One* 2010, **5**:e13250.
18. Buchan JR, Parker R: **Eukaryotic stress granules: the ins and outs of translation.** *Mol Cell* 2009, **36**:932-941.
19. Colombrita C, Zennaro E, Fallini C, Weber M, Sommacal A, Buratti E, Silani V, Ratti A: **TDP-43 is recruited to stress granules in conditions of oxidative insult.** *J Neurochem* 2009, **111**:1051-1061.
20. Dewey CM, Cenik B, Sephton CF, Dries DR, Mayer Pr, Good SK, Johnson BA, Herz J, Yu G: **TDP-43 is directed to stress granules by sorbitol, a novel physiological osmotic and oxidative stressor.** *Mol Cell Biol* 2010, **31**:1098-108.
21. Moisse K, Volkening K, Leystra-Lantz C, Welch I, Hill T, Strong MJ: **Divergent patterns of cytosolic TDP-43 and neuronal progranulin expression following axotomy: implications for TDP-43 in the physiological response to neuronal injury.** *Brain Res* 2009, **1249**:202-211.
22. Volkening K, Leystra-Lantz C, Yang W, Jaffee H, Strong MJ: **Tar DNA binding protein of 43 kDa (TDP-43), 14-3-3 proteins and copper/zinc superoxide dismutase (SOD1) interact to modulate NFL mRNA stability. Implications for altered RNA processing in amyotrophic lateral sclerosis (ALS).** *Brain Res* 2009, **1305**:168-182.
23. Ito D, Seki M, Tsunoda Y, Uchiyama H, Suzuki N: **Nuclear transport impairment of amyotrophic lateral sclerosis-linked mutations in FUS/TLS.** *Ann Neurol* 2011, **69**:152-162.
24. Dormann D, Rodde R, Edbauer D, Bentmann E, Fischer I, Hruscha A, Than ME, Mackenzie IR, Capell A, Schmid B, Neumann M, Haass C: **ALS-associated fused in sarcoma (FUS) mutations disrupt Transportin-mediated nuclear import.** *EMBO J* 2010, **29**:2841-2857.
25. Freibaum BD, Chitta RK, High AA, Taylor JP: **Global analysis of TDP-43 interacting proteins reveals strong association with RNA splicing and translation machinery.** *J Proteome Res* 2010, **9**:1104-1120.
26. Barber SC, Mead RJ, Shaw PJ: **Oxidative stress in ALS: A mechanism of neurodegeneration and a therapeutic target.** *Biochim Biophys Acta* 2006, **1762**:1051-1067.
27. Nonaka T, Arai T, Buratti E, Baralle FE, Akiyama H, Hasegawa M: **Phosphorylated and ubiquitinated TDP-43 pathological inclusions in ALS and FTLD-U are recapitulated in SH-SY5Y cells.** *FEBS Lett* 2009, **583**:394-400.
28. Caragounis A, Price KA, Soon CP, Filiz G, Masters CL, Li QX, Crouch PJ, White AR: **Zinc induces depletion and aggregation of endogenous TDP-43.** *Free Radic Biol Med* 2010, **48**:1152-1161.
29. Dormann D, Capell A, Carlson AM, Shankaran SS, Rodde R, Neumann M, Kremmer E, Matsuwaki T, Yamanouchi K, Nishihara M, Haass C: **Proteolytic processing of TAR DNA binding protein-43 by caspases produces C-terminal fragments with disease defining properties independent of progranulin.** *J Neurochem* 2009, **110**:1082-1094.
30. Nishimoto Y, Ito D, Yagi T, Nihei Y, Tsunoda Y, Suzuki N: **Characterization of alternative isoforms and inclusion body of the TAR DNA-binding protein-43.** *J Biol Chem* 2010, **285**:608-619.
31. Chang JW, Koike T, Iwashima M: **hnRNP-K is a nuclear target of TCR-activated ERK and required for T-cell late activation.** *Int Immunol* 2009, **21**:1351-1361.
32. Zhou R, Shanas R, Nelson MA, Bhattacharyya A, Shi J: **Increased expression of the heterogeneous nuclear ribonucleoprotein K in pancreatic cancer and its association with the mutant p53.** *Int J Cancer* 2010, **126**:395-404.
33. Buxade M, Parra JL, Rousseau S, Shpiro N, Marquez R, Morrice N, Bain J, Espel E, Proud CG: **The Mnks are novel components in the control of TNF alpha biosynthesis and phosphorylate and regulate hnRNP A1.** *Immunity* 2005, **23**:177-189.
34. Habelhah H, Shah K, Huang L, Ostareck-Lederer A, Burlingame AL, Shokat KM, Hentze MW, Ronai Z: **ERK phosphorylation drives cytoplasmic accumulation of hnRNP-K and inhibition of mRNA translation.** *Nat Cell Biol* 2001, **3**:325-330.
35. Shimada N, Rios I, Moran H, Sayers B, Hubbard K: **p38 MAP kinase-dependent regulation of the expression level and subcellular distribution of heterogeneous nuclear ribonucleoprotein A1 and its involvement in cellular senescence in normal human fibroblasts.** *RNA Biol* 2009, **6**:293-304.
36. Guil S, Long JC, Caceres JF: **hnRNP A1 relocalization to the stress granules reflects a role in the stress response.** *Mol Cell Biol* 2006, **26**:5744-5758.
37. Bogoyevitch MA, Ngoei KR, Zhao TT, Yeap YY, Ng DC: **c-Jun N-terminal kinase (JNK) signaling: recent advances and challenges.** *Biochim Biophys Acta* 2010, **1804**:463-745.

38. Yang W, Tiffany-Castiglioni E, Koh HC, Son IH: **Paraquat activates the IRE1/ASK1/JNK cascade associated with apoptosis in human neuroblastoma SH-SY5Y cells.** *Toxicol Lett* 2009, **191**:203-210.
39. Choi WS, Abel G, Klintworth H, Flavell RA, Xia Z: **JNK3 mediates paraquat- and rotenone-induced dopaminergic neuron death.** *J Neuropathol Exp Neurol* 2010, **69**:511-520.
40. Stebbins JL, De SK, Machleidt T, Becattini B, Vazquez J, Kuntzen C, Chen LH, Cellitti JF, Riel-Mehan M, Emdadi A, Solinas G, Karin M, Pellecchia M: **Identification of a new JNK inhibitor targeting the JNK-JIP interaction site.** *Proc Natl Acad Sci USA* 2008, **105**:16809-16813.
41. Wasserman T, Katsenelson K, Daniliuc S, Hasin T, Choder M, Aronheim A: **A novel c-Jun N-terminal kinase (JNK)-binding protein WDR62 is recruited to stress granules and mediates a nonclassical JNK activation.** *Mol Biol Cell* 2010, **21**:117-130.
42. Buratti E, Brindisi A, Giombi M, Tisminetzky S, Ayala YM, Baralle FE: **TDP-43 binds heterogeneous nuclear ribonucleoprotein A/B through its C-terminal tail: an important region for the inhibition of cystic fibrosis transmembrane conductance regulator exon 9 splicing.** *J Biol Chem* 2005, **280**:37572-37584.
43. Habelhah H, Shah K, Huang L, Burlingame AL, Shokat KM, Ronai Z: **Identification of new JNK substrate using ATP pocket mutant JNK and a corresponding ATP analogue.** *J Biol Chem* 2001, **276**:18090-18095.
44. Hostetter C, Licata LA, Witkiewicz A, Costantino CL, Yeo CJ, Brody JR, Keen JC: **Cytoplasmic accumulation of the RNA binding protein HuR is central to tamoxifen resistance in estrogen receptor positive breast cancer cells.** *Cancer Biol Ther* 2008, **7**:1496-1506.
45. D'Ambrogio A, Buratti E, Stuani C, Guarnaccia C, Romano M, Ayala YM, Baralle FE: **Functional mapping of the interaction between TDP-43 and hnRNP A2 in vivo.** *Nucleic Acids Res* 2009, **37**:4116-4126.
46. Perlson E, Jeong GB, Ross JL, Dixit R, Wallace KE, Kalb RG, Holzbaur EL: **A switch in retrograde signaling from survival to stress in rapid-onset neurodegeneration.** *J Neurosci* 2009, **29**:9903-9917.
47. Zhu X, Perry G, Smith MA: **Amyotrophic lateral sclerosis: a novel hypothesis involving a gained 'loss of function' in the JNK/SAPK pathway.** *Redox Rep* 2003, **8**:129-133.
48. Veglianese P, Lo Coco D, Bao Cutrona M, Magnoni R, Pennacchini D, Pozzi B, Gowing G, Julien JP, Tortarolo M, Bendotti C: **Activation of the p38MAPK cascade is associated with upregulation of TNF alpha receptors in the spinal motor neurons of mouse models of familial ALS.** *Mol Cell Neurosci* 2006, **31**:218-231.
49. Kim EK, Choi EJ: **Pathological roles of MAPK signaling pathways in human diseases.** *Biochim Biophys Acta* 2010, **1802**:396-405.
50. Atzori C, Ghetti B, Piva R, Srinivasan AN, Zolo P, Delisle MB, Mirra SS, Migheli A: **Activation of the JNK/p38 pathway occurs in diseases characterized by tau protein pathology and is related to tau phosphorylation but not to apoptosis.** *J Neuropathol Exp Neurol* 2001, **60**:1190-1197.
51. Ayala V, Granado-Serrano A, Cacabelos D, Naudí A, Ilieva V, Boada J, Caraballo-Miralles V, Lladó J, Ferrer I, Pamplona R, Portero-Otin M: **Cell stress induces TDP-43 pathological changes associated with ERK1/2 dysfunction: implications in ALS.** *Acta Neuropathol* 2011.
52. Migheli A, Piva R, Atzori C, Troost D, Schiffer D: **c-Jun, JNK/SAPK kinases and transcription factor NF-kappa B are selectively activated in astrocytes, but not motor neurons, in amyotrophic lateral sclerosis.** *J Neuropathol Exp Neurol* 1997, **56**:1314-1322.
53. Stevenson A, Yates DM, Manser C, De Vos KJ, Vagnoni A, Leigh PN, McLoughlin DM, Miller CC: **Riluzole protects against glutamate-induced slowing of neurofilament axonal transport.** *Neurosci Lett* 2009, **454**:161-164.

doi:10.1186/1750-1326-6-57
Cite this article as: Meyerowitz *et al.*: C-Jun N-terminal kinase controls TDP-43 accumulation in stress granules induced by oxidative stress. *Molecular Neurodegeneration* 2011 6:57.

The FASEB Journal • Research Communication

Phosphorylated α-synuclein can be detected in blood plasma and is potentially a useful biomarker for Parkinson's disease

Penelope G. Foulds,* J. Douglas Mitchell,‡ Angela Parker,‡ Roisin Turner,‡ Gerwyn Green,† Peter Diggle,† Masato Hasegawa,§ Mark Taylor,* David Mann,‖ and David Allsop*,[1]

*Division of Biomedical and Life Sciences and †Division of Health Research, School of Health and Medicine, University of Lancaster, Lancaster, UK; ‡Royal Preston Hospital, Preston, UK; §Department of Molecular Neurobiology, Tokyo Institute of Psychiatry, Tokyo, Japan; and ‖Neurodegeneration and Mental Health Research Group, School of Community-Based Medicine, University of Manchester, Hope Hospital, Salford, UK

ABSTRACT **Parkinson's disease (PD) is characterized by the presence of Lewy bodies containing phosphorylated and aggregated α-synuclein (α-syn). α-Syn is present in human body fluids, including blood plasma, and is a potential biomarker for PD. Immunoassays for total and oligomeric forms of both normal and phosphorylated (at Ser-129) α-syn have been used to assay plasma samples from a longitudinal cohort of 32 patients with PD (sampled at mo 0, 1, 2, 3), as well as single plasma samples from a group of 30 healthy control participants. The levels of α-syn in plasma varied greatly between individuals, but were remarkably consistent over time within the same individual with PD. The mean level of phospho-α-syn was found to be higher (P=0.053) in the PD samples than the controls, whereas this was not the case for total α-syn (P=0.244), oligo-α-syn (P=0.221), or oligo-phospho-α-syn (P=0.181). Immunoblots of plasma revealed bands (at 21, 24, and 50–60 kDa) corresponding to phosphorylated α-syn. Thus, phosphorylated α-syn can be detected in blood plasma and shows more promise as a diagnostic marker than the nonphosphorylated protein. Longitudinal studies undertaken over a more extended time period will be required to determine whether α-syn can act as a marker of disease progression.—Foulds, P. G., Mitchell, J. D., Parker, A., Turner, R., Green, G., Diggle, P., Hasegawa, M., Taylor, M., Mann, D., Allsop, D. Phosphorylated α-synuclein can be detected in blood plasma and is potentially a useful biomarker for Parkinson's disease. *FASEB J.* 25, 4127–4137 (2011). www.fasebj.org**

Key Words: Lewy body · oligomer · immunoassay · immunoblot

PARKINSON'S DISEASE (PD) is the second most common neurodegenerative disorder after Alzheimer's disease (AD) and is characterized clinically by the 3 cardinal motor symptoms of resting tremor, rigidity, and bradykinesia. Patients often exhibit further symptoms, including postural imbalance, gait disturbance, and a mask-like facial expression. In the advanced stages of PD, nonmotor symptoms can also appear, including anxiety, depression, dementia, and psychosis. The defining neuropathological features of idiopathic PD are the loss of dopaminergic neurons from the substantia nigra (SN) and the presence of Lewy bodies (LBs) and Lewy neurites (LNs) in surviving neurons of this and other brain regions (1). Similar lesions are present within the cerebral cortex in the related disorder of dementia with Lewy bodies (DLB; ref. 2). LBs and LNs contain a misfolded, fibrillar, and phosphorylated form of the protein α-synuclein (α-syn; refs. 1, 3). Pathological changes involving α-syn, chiefly in glial cells, also occur in multiple system atrophy (MSA), and, therefore, PD, DLB, and MSA are often collectively referred to as "α-syncleinopathies" (2). Duplication (4, 5), triplication (6), and mutation (7–9) of the gene encoding α-syn (*SNCA*) are all causes of hereditary forms of either PD or DLB. α-Syn oligomers are believed to be toxic to cells, as are oligomers derived from the various proteins associated with several other protein-misfolding neurodegenerative disorders, such as AD or the prion disorders (10, 11). Overexpression of wild-type or mutant α-syn in animal models can produce a phenotype resembling PD, including SN degeneration, movement problems and responsiveness to L-dopa therapy (12–15). Together, these observations suggest that α-syn plays a pivotal role in the development of the α-synucleinopathies (16).

PD is one of several neurological movement disor-

[1] Correspondence: Division of Biomedical and Life Sciences, School of Health and Medicine, University of Lancaster, Lancaster, LA1 4AY, UK. E-mail: d.allsop@lancaster.ac.uk

doi: 10.1096/fj.10-179192

This article includes supplemental data. Please visit *http://www.fasebj.org* to obtain this information.

ders that can produce similar symptoms, and a correct diagnosis is critically dependent on clinical examination to rule out disorders that can mimic PD. A diagnosis of PD is considered if the person exhibits more than one of the 3 cardinal motor symptoms mentioned above (17). The presence of resting tremor supports the diagnosis of PD more than the other two symptoms, but ~20% of patients with autopsy-confirmed PD fail to develop any resting tremor (18). Moreover, only 69–70% of people with autopsy-confirmed PD have at least two of the cardinal signs of the disease and 20–25% of people with two of these symptoms have a pathological diagnosis other than PD (19, 20). Perhaps even more surprising is the finding that 13–19% of people who demonstrate all three of the cardinal features have a pathological diagnosis other than PD (19, 20). Because the progression of neurological movement disorders and their treatment varies greatly, proper clinical diagnosis is essential for correct patient management. Furthermore, by the time PD is diagnosed, >60% of dopaminergic neurons in the SN can already be lost (21), making accurate early diagnosis, ideally before clinical symptoms appear, essential for any effective neuroprotective intervention strategy. Also, the clinical diagnosis of early PD may be difficult because although the patient might complain of symptoms suggesting PD, the neurological examination may be normal (22). These problems with clinical diagnosis have led to an increased interest in the development of diagnostic markers for PD, including advanced brain imaging methodologies (23) and molecular biomarkers (24). Genetic testing for mutations in genes linked to familial PD (including *SNCA*) is available (25), but it is only relevant when there is a strong family history, or when symptoms present at an unusually young age.

We have reported that α-syn is released from cells and is present in human body fluids, including cerebrospinal fluid (CSF) and blood plasma (26). This extracellular form of α-syn seems to be secreted from neuronal cells by exocytosis (27, 28) and could play an important role in cell-to-cell transfer of α-syn pathology in the brain (29). There is now an emerging consensus that the levels of α-syn are, on average, lower in samples of CSF taken from a group of patients with PD compared with a group of normal or neurological controls (30, 31), especially when the confounding variables of age and blood contamination are taken into account (32, 33). However, obtaining CSF is an invasive procedure, and analysis of α-syn levels in CSF is not generally amenable to longitudinal study. There are also some studies of α-syn as a potential biomarker in the much more accessible peripheral blood, with an initial report suggesting increased levels of this protein in plasma samples from patients with PD compared with those from healthy controls (34). However, subsequent studies have reported decreased levels of α-syn in PD plasma (35) or no significant change (36). We have shown that the levels of oligomeric α-syn appear to be significantly elevated in plasma samples from a group of patients with PD compared with a group of diseased controls (37). To develop this line of enquiry further, we have now set up a longitudinal study in newly diagnosed patients with PD to examine the levels of various different forms of α-syn, including phosphorylated and/or oligomeric forms, in blood plasma. Because α-syn accumulates in a phosphorylated and aggregated form in LBs (3), it is possible that these modified, pathological forms of the protein will more accurately reflect the fundamental neuropathology of PD than straightforward measures of "total" α-syn (33, 38). Our ultimate aim is to develop a relatively simple test for the early diagnosis of PD, or a surrogate marker for monitoring the progression of PD. Here, we report the results obtained during the initial phase of this longitudinal study.

MATERIALS AND METHODS

Patient population and clinical method

Participants for this study were recruited (with ethical approval, using appropriate consenting procedures) from the neurological service based at the Royal Preston Hospital along with other similar departments in the northwest of England. The diagnosis of PD was based on the UK Parkinson's Disease Society diagnostic criteria for PD (39). Severity of disease was defined in terms of patients satisfying the criteria for stages 1 or 2 on the Hoehn and Yahr scale.

The overall target for the study was to follow a cohort of 200 patients meeting these criteria over a period of 2–3 yr, reviewing them at 4- to 6-mo intervals. This study is ongoing, but the plan was also to follow the first 32 patients more intensively over the initial phases of the study, and this group was seen at monthly intervals for the first 3 mo. The results from these 32 patients over the first 3 mo are presented here. Blood samples were obtained from the participating sites (Preston and Arrowe Park). Around 3 ml of blood was collected in tubes containing EDTA, and the plasma was separated within 3 h by centrifuging the blood at 3000 *g* for 10 min. The plasma was immediately stored at −80°C. Appropriate care was taken to avoid contamination of the plasma samples with cells or components of the pellet obtained from the centrifugation. The samples were thawed at room temperature directly before analysis. Repeated freeze/thaw cycles were avoided.

Control subjects were healthy individuals with no apparent neurological or known psychiatric symptoms who were the spouses of patients attending the Cerebral Function Unit clinics at Hope Hospital (Salford Royal Hospital, National Health Service Foundation Trust) for investigation and diagnosis of dementia. These control subjects were recruited as part of an ongoing investigation into the genetics and molecular biology of dementia approved by the Oldham Local Research Ethics Committee. Blood plasma was prepared and stored as described above.

Preparation of recombinant α-syn

Recombinant α-syn (without any purification tag) was prepared at Lancaster University from *Escherichia coli* using the following protocol. pJEK2 was used to transform FB850, a *rec* A^- derivative of BL21 (DES) pLysS. FB850 carrying this plasmid was grown in an 800-ml batch culture, and protein expression was induced through the addition of isopropyl-β-

D-thiogalactopyranoside (IPTG). A protein with a molecular weight of ~17 kDa started to accumulate in the cells 30 min after induction and reached maximum levels after 150 min. Immunoblot analysis identified this protein as α-syn using an anti-α-syn mouse monoclonal antibody (MAb 211; Santa Cruz Biotechnology, Santa Cruz, CA, USA). After a 3-h induction, the suspension was centrifuged, and the cells were resuspended in buffer. The cells were lysed by sonication, and then cell debris and insoluble material were removed by centrifugation at 4°C for 1 h at 30,000 rpm. α-Syn was extracted from the supernatant by ammonium sulfate precipitation, then purified using two chromatography columns; mono Q and Superdex 200 (Amersham Biosciences, Piscataway, NJ, USA). After purification, 5 μg of protein ran as a single band when observed on a Coomassie blue-stained SDS gel, corresponding to monomeric α-syn.

Preparation of phosphorylated recombinant α-syn

Phosphorylated α-syn was prepared from recombinant α-syn, as described previously (40). Briefly, α-syn (630 μM) was incubated with casein kinase II (CK2; New England Biolabs, Ipswitch, MA, USA) in 1 ml of buffer containing 20 mM Tris-HCl (pH 7.5), 50 mM KCl, 10 mM $MgCl_2$, and 1 mM ATP at 30°C for 24 h. For effective phosphorylation, CK2 was added to the reaction mixture at 2-h intervals for the first 10 h (7500 U×5). The reaction was stopped by boiling for 5 min, cleared by centrifugation at 113,000 *g* for 20 min at 4°C, and then loaded onto a Resource Q anion-exchange column (Amersham Biosciences) equilibrated with 20 mM Tris-HCl (pH 8.0) and 0.2 M NaCl, and then eluted with a linear gradient of NaCl from 0.20 to 0.35 M for 15 min at a flow rate of 1 ml/min. Fractionated samples were analyzed by immunoblotting with a phosphorylation-dependent anti-α-syn antibody, PSer129 (Epitomics, Burlingame, CA, USA), and mass spectrometry. The PSer129-positive phosphorylated α-syn recovered in the fractions with ~0.3 M NaCl was concentrated by ammonium sulfate precipitation.

Preparation of oligomeric forms of recombinant α-syn

To prepare a standard for the oligomeric α-syn immunoassay, the recombinant protein was oligomerized by incubation at 45 μM in PBS in an orbital shaker at 37°C for 5 d, and the monomer and oligomer were separated by size-exclusion chromatography. A sample (0.5 ml) of preaggregated α-syn was loaded onto a Superdex 200 column (44×1 cm) connected to a fast protein liquid chromatography (FPLC) system (Atka Purifier; GE Healthcare, New York, NY, USA) and eluted with running buffer (PBS) at a flow rate of 0.5 ml/min. Absorbance of the eluate was monitored at 280 nm; fractions of 1 ml were collected, and protein concentration was determined.

To prepare a standard for the oligo-phospho-α-syn immunoassay, the phosphorylated protein was oligomerized by incubation at 50 μM in PBS in an orbital shaker at 37°C for 5 d. Aggregation of the protein was confirmed by thioflavin T assay. In this case, the amount of sample available was too small to fractionate by size-exclusion chromatography.

Immunoassay methods

We have already established immunoassay methods for the measurement of total and soluble oligomeric forms of α-syn in human biological fluids, including blood plasma (37, 41), and these methods have been further optimized.

Total α-syn

A 96-well microtiter plate (Iwaki, Holliston, MA, USA) was coated with 100 μl/well of anti-α-syn monoclonal antibody 211 diluted 1:1000 (0.2 μg/ml; Santa Cruz Biotechnology) in 50 mM $NaHCO_3$ (pH 9.6) and incubated at 4°C overnight. The wells were then washed 4 times with PBS containing 0.05% Tween-20 (PBS-T) and were incubated for 2 h at 37°C with 200 μl/well of freshly prepared blocking buffer (2.5% gelatin in PBS-T). The plate was washed again 4 times with PBS-T, and 100 μl of the assay standard or plasma samples was added to each well (each plasma sample was diluted 1:40 with PBS), and the assays were performed in triplicate. Following this, the plate was incubated at 37°C for 2 h. After a repeat washing with PBS-T, 100 μl/well of the detection antibody, anti-α/β/γ-synuclein FL-140 (Santa Cruz Biotechnology), dilution 1:750 (0.27 μg/ml) in blocking buffer was added, and the plate was incubated at 37°C for 2 h. After another wash with PBS-T, the plate was incubated with 100 μl/well of secondary antibody [goat anti-rabbit horseradish peroxidase (HRP); Sigma, St. Louis, MO, USA], dilution 1:10,000 in blocking buffer at 37°C for 2 h. The plate was then washed again with PBS-T before adding 100 μl/well of Sure Blue TMB microwell peroxidase substrate (KPL, Gaithersburg, MD, USA) and leaving the color to develop for 30 min at room temperature. Finally 100 μl/well of stop solution (0.3 M H_2SO_4) was added, and absorbance at 450 nm was determined. Recombinant monomeric α-syn was used to create a standard curve.

Oligomeric α-syn (oligo-α-syn)

The microtiter plate was coated and blocked using the same method as the assay for total α-syn. The wells were then washed 4 times with PBS-T, and 100 μl of the plasma sample (diluted 1:25 with PBS) or assay standard (oligo-α-syn) was added to each well, in triplicate. Following this, the plate was incubated at 37°C for 2 h. After a repeat wash with PBS-T, 100 μl/well of the detection antibody, biotinylated anti-α-synuclein 211 (diluted 1:1000 in blocking buffer) was added, and the plate was incubated at 37°C for 2 h. After another wash with PBS-T, the plate was incubated with 100 μl/well of streptavidin-europium, diluted 1:500 in streptavidin-europium buffer (Perkin Elmer, Wellesley, MA, USA) and shaken for 10 min. After a further 50-min agitation on a rotating platform, the plate was washed again with PBS-T, before adding 100 μl/well enhancer solution (Perkin Elmer). Finally, the plates were read on a Wallac Victor^2 1420 multilabel plate reader (Perkin Elmer), using the time-resolved fluorescence setting for europium.

Total phosphorylated α-syn (pS-α-syn)

The antibody-sandwich ELISA for total α-syn was modified to detect only the protein phosphorylated at Ser-129 by replacing the 211 phospho-independent capture antibody with polyclonal anti-α-synuclein N-19 (Santa Cruz Biotechnology), diluted 1:3,000 (0.07 μg/ml). The phospho-dependent rabbit monoclonal antibody, Phospho (pS129) antibody (Epitomics), used at a dilution of 1:3000, was the chosen detection antibody. This antibody detects only α-syn phosphorylated at Ser-129. The preferred secondary antibody was human serum absorbed goat anti-rabbit HRP, 1:3000 (KPL), rehydrated in 1 ml H_2O. Recombinant pS-α-syn was used as the assay standard.

Oligomeric phosphorylated α-syn (oligo-pS-α-syn)

The antibody-sandwich immunoassay for oligo-α-syn was modified to detect only phosphorylated, oligomeric forms of the

protein, by replacing the 211 phospho-independent capture antibody with the phospho-dependent rabbit monoclonal antibody, pS129 (Epitomics), used at a dilution of 1:3000. The detection antibody was biotinylated pS129 at a dilution of 1:400. Recombinant oligo-pS-α-syn was used to generate a standard curve.

Preparation of biotinylated antibodies

To prepare the biotinylated antibody, 200 g Sulfo-NHS-LC-Biotin (Pierce, Rockford, IL, USA) was reacted with the required antibody (1 ml, 200 μg/ml) in PBS and then placed on ice for 2 h. The mixture was desalted on Bio-Spin-6 columns (Bio-Rad, Richmond, CA, USA) to remove excess uncoupled biotin and the biotinylated antibody was stored at −20°C until use.

Immunocapture of α-syn from plasma

Dynabeads covalently coupled with recombinant protein G were derivatized with goat polyclonal anti-α-syn synuclein N-19 antibody (Santa Cruz Biotechnology), as recommended by the manufacturer (Dynal Biotech, Wirral, UK). Plasma (500 μl) was added to the beads and incubated overnight at 4°C. The plasma samples were chosen according to the immunoassay results, with one sample giving a high signal for the phosphorylated protein, the other a low signal, and a control containing PBS only. The beads were then washed 3 times with 0.1 M phosphate buffer (pH 8.2). Any captured protein was eluted from the beads by boiling for 10 min in NuPAGE LDS sample buffer (Invitrogen, Carlsbad, CA, USA) and was examined by gel electrophoresis and immunoblotting.

Gel electrophoresis and immunoblotting

The protein eluted from the magnetic Dynabeads was separated on 12.5% acylamide gels. The separated proteins were transferred to nitrocellulose membranes (0.45 μm, Invitrogen) at 30 V, 125 mA for 1 h. Membranes were blocked with 5% dried skimmed milk dissolved in PBS-Tween (PBST), for 1 h. The membranes were probed overnight at 4°C with either phospho-dependent rabbit anti-α-synuclein monoclonal antibody pS129 (Epitomics) at a dilution of 1:5000; rabbit polyclonal anti-synuclein antibody FL-140 (Santa Cruz Biotechnology) at a dilution of 1:1000 (0.2 μg/ml); or rabbit anti-ubiquitin antibody FL-76 (Santa Cruz Biotechnology) at a dilution of 1:1000 (0.2 μg/ml) in PBST. The membranes were washed 3 times in PBST, followed by incubation with human serum absorbed HRP-conjugated goat anti-rabbit (Sigma), 1:10,000 in PBST, for 1 h. The protein bands were visualized using ECL reagents (Pierce), as described by the manufacturer.

Analysis of immunoassay data

A set of standards for one of the 4 different assays (*i.e.*, for total α-syn, oligo-α-syn, pS-α-syn, or oligo-pS-α-syn) was included on each microtiter plate, as appropriate for the type of protein being measured on that plate. Standard curves were fitted using nonlinear least squares (see **Fig. 1** for representative examples of standard curves for each of the four different immunoassays). The samples of blood plasma from

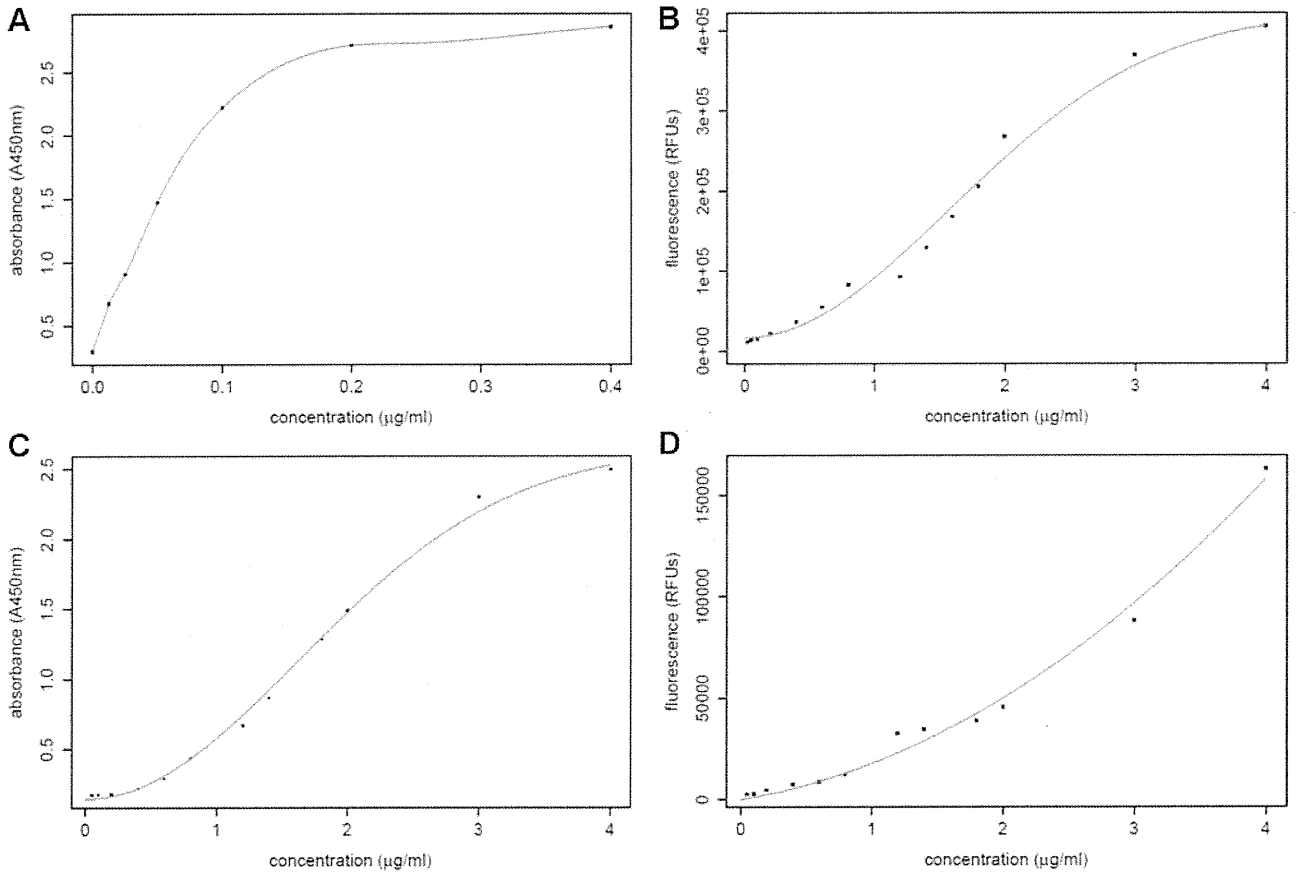

Figure 1. Examples of standard curves obtained for total α-syn (*A*), oligo-α-syn (*B*), pS-α-syn (*C*) and oligo-pS-α-syn (*D*). These are representative curves, each obtained from a single ELISA plate.

patients with PD and controls, diluted as indicated above, were measured in triplicate for each individual at each time point. The standard curves for each individual plate were used to transform the absorbance values (total α-syn, pS-α-syn) or relative fluorescence units (RFU; oligo-α-syn, oligo-pS-α-syn) for that particular plate into protein concentrations, and, in this way, any variation between plates was accounted for. The specificity of the oligo-α-syn immunoassay toward aggregated forms of α-syn has been reported previously (37, 41) but was confirmed here by analysis of fractions obtained by gel filtration of preaggregated, recombinant α-syn; only the peak containing α-syn oligomers, and not the monomer peak, was detected by the oligo-α-syn immunoassay. Also, as expected, the nonphosphorylated form of α-syn gave no signal in the pS-α-syn immunoassay, and the oligo-pS-α-syn immunoassay detected only pS-α-syn that had been preaggregated (data not shown). Further, when the blood plasma samples were immunodepleted with anti-α-syn antibodies C211 or FL-140, each coupled to magnetic Dynabeads, and then tested in the immunoassays, only trace signals could be detected above background compared to the nonimmunodepleted samples (data not shown).

To investigate whether the protein levels changed over time (*i.e.*, during the first 3 mo) a linear mixed model was fitted to the longitudinal data from each assay (details in Supplemental Data).

A classic 2-sample *t* test was used to determine whether there was any significant difference between the mean levels of each of the different forms of α-syn when comparing the plasma samples from the patients with PD with those from the healthy controls. To better satisfy the assumptions underlying this test, the empirical distributions were constructed on the logarithmic scale to obtain a more symmetric distribution than was obtained on the original scale.

RESULTS

Patient population and demographics

Demographic details of the cohort of 32 patients with PD that was followed at monthly intervals for 3 mo are summarized in **Table 1**. The mean age of this cohort on ascertainment and initial sampling was 68.2 yr (youngest 56 yr, oldest 85 yr). Among the 30 recruited healthy controls, there were 13 males and 17 females, with a median age of 63 yr and mean age of 61.5 yr (youngest 42 yr, oldest 75 yr). The PD case and control subjects were recruited in parallel, at the same clinical centers, and the blood samples were taken and processed by the same personnel at each site. Moreover, the plasma samples were effectively randomized for analysis, with both control and PD samples being assayed together on the same microtiter plates.

TABLE 1. *Demographic details of the cohort of 32 patients with PD*

Parameter	Value
Gender (male/female)	23/9
Hoehn and Yahr 1.0	5
Hoehn and Yahr 1.5	3
Hoehn and Yahr 2.0	24
Median PD onset age (yr)	61.9 (55.5–69.7)
Age at study recruitment (yr)	68.4 (62.3–73.8)
Disease duration at study recruitment (yr)	4.9 (3.1–9.3)

Values in parentheses indicate interquartile range.

Longitudinal data from patients with PD

Figure 2 presents a bar plot of the total α-syn plasma concentrations for each individual with PD over time (*i.e.*, for mo 0, 1, 2, 3) where, within each time point, we have averaged over triplicate measurements. It can be seen that the levels of total α-syn varied greatly between individuals, within an overall range of 0.01–6 μg/ml. Although a few individuals did show small, stepwise increases or decreases of total α-syn levels over this (very short) sampling period (see, for example, patient 32 in Fig. 2*B*), one of the most striking findings from this study was that, overall, the immunoassay results from the repeat PD plasma samples were remarkably consistent within each individual over time. This was a general finding for the results from all four of the different α-syn immunoassays, but it is illustrated here (Fig. 2) for the total-α-syn data only. Data for the other 3 assays (Supplemental File S2), together with a linear mixed model-based analysis (Supplemental File S1) for all 4 α-syn assays, are available in Supplemental Data. From the latter analysis, it is clear that the variation in α-syn levels across time within an individual is negligible relative to the variation across individuals. The model specifies a time trend, in addition to accounting for inherent differences in protein levels between individuals and differences across time within an individual. In all cases, the confidence interval for the estimated temporal effect covered 0. Thus, we conclude that there was no significant change over time for the levels of α-syn being measured by any of the immunoassays.

Comparison of patients with PD and controls

Empirical distributions of the α-syn concentrations for each assay were highly skewed on the original scale. **Figure 3** presents box plots pertaining to each assay, stratified according to patients with PD and controls. Note that the whiskers of the box plots extend by no more than the range of the data (largest minus smallest value) multiplied by the interquartile range. Extending the whiskers to the largest and smallest values would yield a rather compressed box. An apparent feature of the box plots is that the median concentration of α-syn for the patients exceeds that of the controls for both of the assays for phosphorylated α-syn (*i.e.*, pS-α-syn in Fig. 3*B*, and oligo-pS-α-syn in Fig. 3*D*). The reverse is true regarding the nonphosphorylated assays (total-α-syn in Fig. 3*A* and oligo-α-syn in Fig. 3*C*). Further, the interquartile range (*i.e.*, box height) reports that the concentrations are far less dispersed for controls compared to patients for both of the phosphorylated α-syn assays. For the nonphosphorylated assays, the controls display a larger spread of concentrations.

To investigate the potential of α-syn as a means of

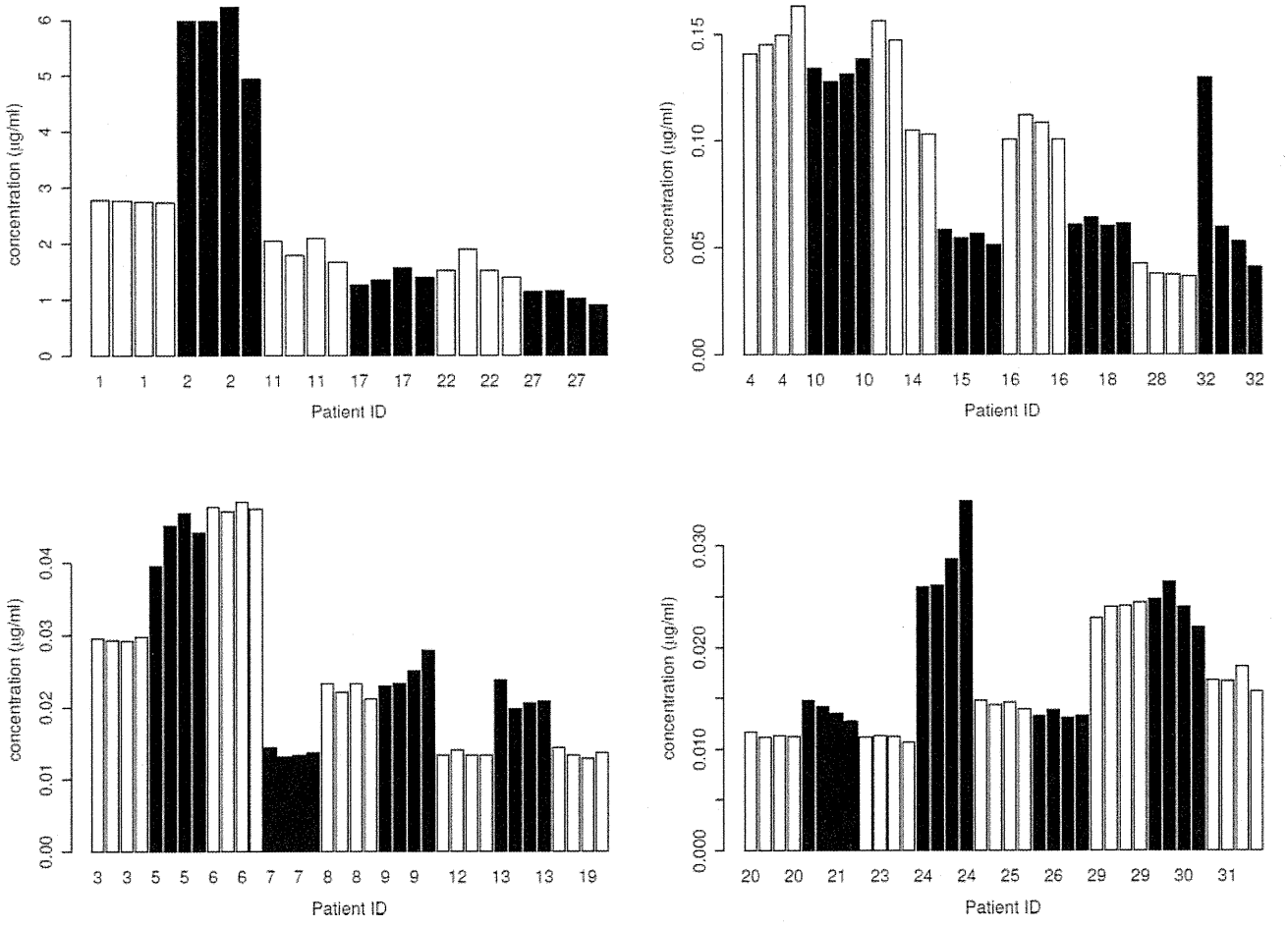

Figure 2. Longitudinal data for the levels of total α-syn in plasma samples from all of the 32 patients with PD. Consecutive bars for each patient represent the level of total α-syn in blood plasma samples taken at 0, 1, 2 and 3 mo. The participants are assigned to one of the 4 sections depending on their overall levels of protein.

discriminating between patients with PD and controls, we determined whether there was any significant difference between the average level of α-syn (on the logarithmic scale) across patients and controls, within all 4 α-syn assays. Because there was no consistent change in α-syn levels over time, nor across replicates within time, in the plasma samples from patients with PD, the concentrations for mo 0, 1, 2 and 3 were averaged over time and replicates in order to obtain a single mean value for each individual patient. Under a classical two-sample t test, the mean level of pS-α-syn was found to be marginally significantly higher for the patients than for the healthy controls (P=0.053). On the other hand, there was no difference across the average levels of patients and controls with regard to total α-syn (P=0.244), oligo-α-syn (P=0.221), or oligo-pS-α-syn (P=0.181).

Association with gender and age

The levels of α-syn showed no association with gender. For the total and oligo-α-syn assays, sampling age was a marginally significant −0.049 (−0.099, −0.001; P=0.052) and significant −0.009 (−0.019, −0.001; P=0.045) predictor, respectively, of α-syn levels in the patients with PD. On the other hand, the P values corresponding to the effect of sampling age on α-syn levels in the patients, under the pS-α-syn and oligo-pS-α-syn assays, were 0.412 and 0.274, respectively. The levels of α-syn showed no correlation with age in the control group. We did also analyze the data adjusting for age, but found no significant effects, and the adjustments did not materially change the (lack of) significance of the relevant assay results. Therefore, we chose to report the unadjusted results for simplicity.

Receiver operating curve (ROC) analysis

Figure 4 displays an ROC curve constructed to evaluate the utility of plasma pS-α-syn levels in discriminating patients with PD from healthy controls. The area under the curve (AUC) of 0.68 suggests that pS-α-syn has some potential value as a discriminant between patients and controls. AUC curves for 2 of the other 3 assays gave AUC values of less than 0.5 (0.28 for total α-syn and 0.22 for oligo-α-syn), which would also indicate a potentially informative result, with plasma levels of these being lower in patients than in controls. An AUC of 0.62 for oligo-pS-α-syn, however, suggests that in this

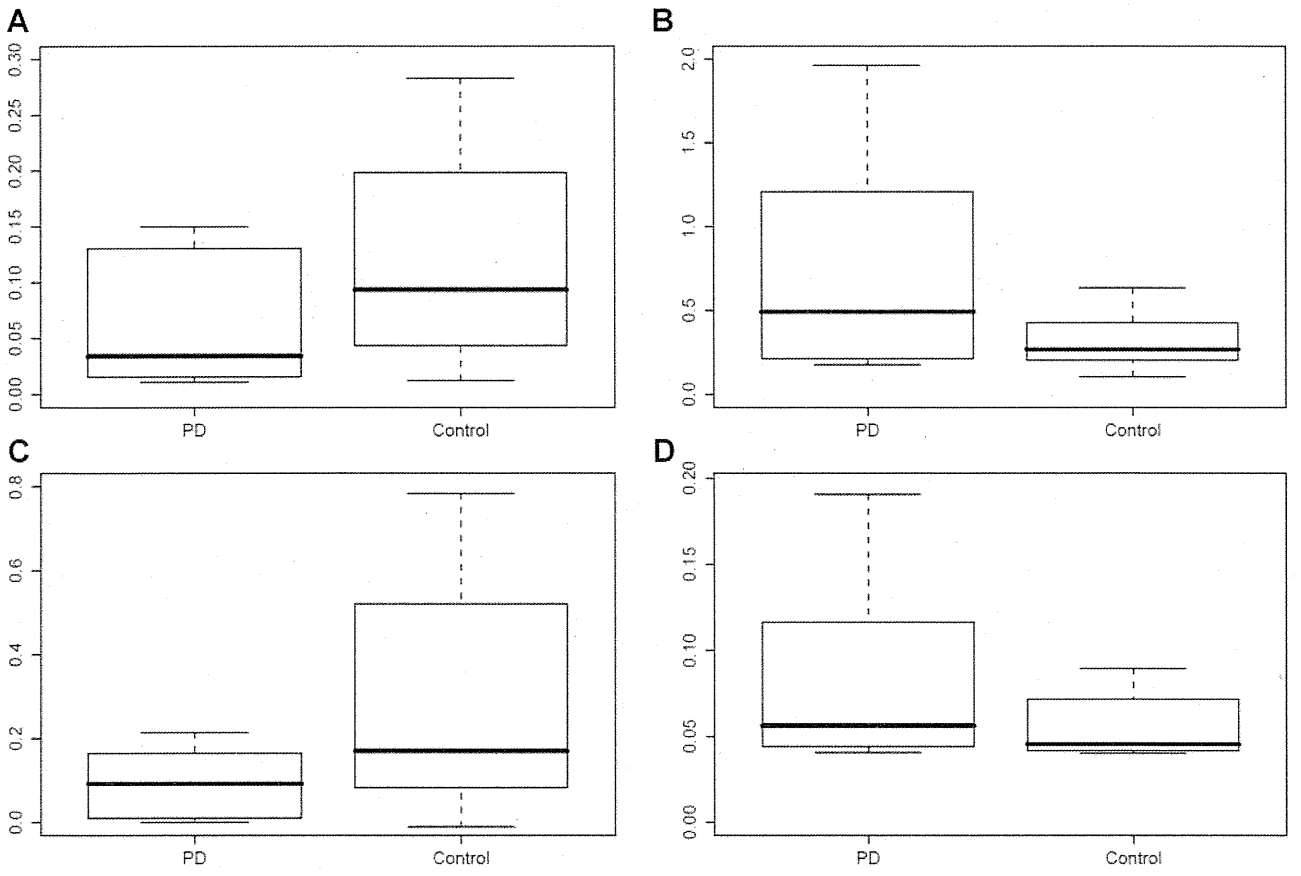

Figure 3. Box plots comparing the levels (in μg/ml) of total α-syn (*A*), pS-α-syn (*B*), oligo-α-syn (*C*), and oligo-pS-α-syn (*D*) in patients with PD compared to healthy controls. In each plot, the box extends from the lower to the upper quartile of the data, with the median indicated by a horizontal line within the box. The difference between the lower and upper quartiles is called the interquartile range (IQR). The upper and lower whiskers extend to the most extreme data values that are no more than 1.5 IQR greater than the upper quartile, and no more than 1.5 IQR less than the lower quartile, respectively.

particular sample set, this assay is less likely to have any practical value as a discriminatory diagnostic tool.

Immunoblot analysis of phosphorylated α-syn in plasma

To better characterize the phosphorylated α-syn detected in plasma, we extracted α-syn from individual PD plasma samples by immunocapture on magnetic Dynabeads and then analyzed the extracted proteins by immunoblotting. The beads were derivatized with the phosphorylation-independent α-syn antibody N-19 (Santa Cruz Biotechnology), which is the antibody used for capture in the pS-α-syn immunoassay. Proteins eluted from the beads were detected by immunoblotting with two different α-syn antibodies: phosphorylation-dependent rabbit monoclonal antibody, pS129, which is the detection antibody used in the pS-α-syn immunoassay (**Fig. 5*A***), and the phosphorylation-independent rabbit polyclonal antibody, FL-140 (Fig. 5*B*). Rabbit anti-ubiquitin antibody FL-76 (Santa Cruz Biotechnology) was used to determine whether any of the bands represented ubiquitinated forms of α-syn (Fig. 5*C*).

The plasma samples were chosen according to the immunoassay results, with one sample giving a low signal for pS-α-syn (Fig. 5, lane 2) and the other a high signal (Fig. 5, lane 3). Immunoblots using the phospho-α-syn-dependent antibody revealed immunoreactive bands from both of these plasma samples, together with the human recombinant phospho-α-syn (at ~17 kDa), but not the nonphosphorylated recombinant protein (Fig. 5*A*, lane 4). The sample derived from the high-reading plasma revealed more intense bands than the low-reading sample, at ~21, 24, and 50–60 kDa. FL-140 revealed both the phosphorylated and nonphosphorylated recombinant protein standards, and also a 24-kDa band in both plasma samples (Fig. 5*B*). The 21-kDa band detected by pS129 was absent, but an additional higher-molecular-weight smear, at >35 kDa, was present. On the basis of the size of these α-syn species, we hypothesize that the 24-kDa band may correspond to phosphorylated, monoubiquitinated α-syn. The anti-ubiquitin antibody, FL-76, strongly labeled the 24-kDa band, as well as the broad "smears" at higher molecular mass, suggesting that all of these bands represent ubiquitinated forms of α-syn (Fig. 5*C*). Control samples of 100 ng human IgG and albumin, the N-19 immunocapture antibody, and a control immunoprecipitation

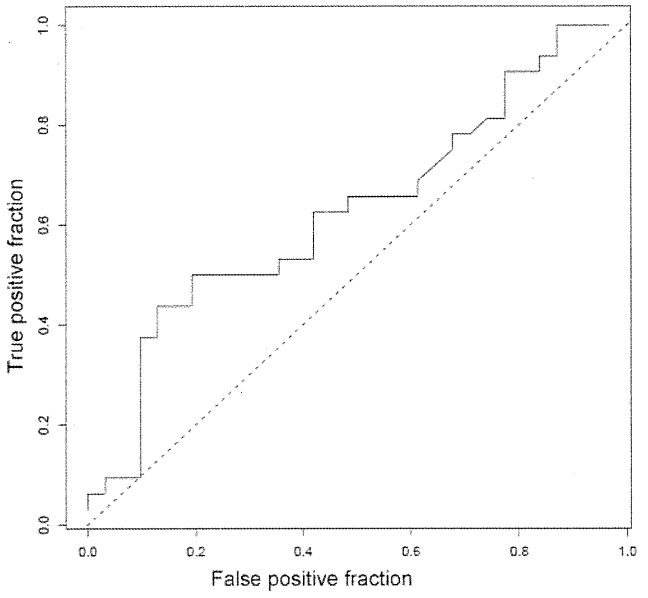

Figure 4. ROC curve showing the ability of the pS-α-syn levels to discriminate between patients with PD and healthy controls (AUC=0.68).

using PBS rather than plasma, gave no immunoreactive bands (data not shown).

DISCUSSION

α-Syn has been linked directly to the etiology of the α-synucleinopathies by mutations in and multiplication of its gene (*SNCA*) that result in familial forms of either PD or DLB. We have reported previously that α-syn is released from cells and is present in human body fluids, including CSF and blood plasma (26). This has led to considerable interest in α-syn in these body fluids as a potential biomarker for the α-synucleinopathies (30–37, 42–44). However, most of these studies have relied on immunoassays that cannot distinguish between monomeric/oligomeric and nonphosphorylated/phosphorylated forms of the protein, apart from two previous studies of oligomeric α-syn in human CSF or blood plasma (37, 44). Here, we have set up individual sandwich immunoassays that can distinguish between total α-syn (MAb 211 capture/ FL-140 detect); oligo-α-syn (Mab 211 capture and detect); pS-α-syn (N19 capture/pS129 detect); and oligo-pS-α-syn (pS129 capture and detect). Our assays for oligomeric forms of α-syn use the double-antibody approach, where the same monoclonal antibody is used for both antigen capture and detection (37, 41). This type of assay cannot detect monomers because the capture antibody occupies the only antibody-binding site available, but it can detect oligomers, because they have multiple binding sites. Our assays for phosphorylated α-syn rely on the specificity of the monoclonal antibody pS129 to α-syn phosphorylated at Ser-129 (45). As anticipated, the recombinant nonphosphorylated α-syn gave no signal in these assays. Although the absorbance/fluorescence values for each of the 4 assays were converted to protein concentrations using the relevant standard curve, due to the nature of these assays, this may only represent an estimate of concentration for that particular assay since the precise nature of the α-syn species detected in plasma has not been not determined for each assay and the native species are likely to differ from the standards prepared from the recombinant

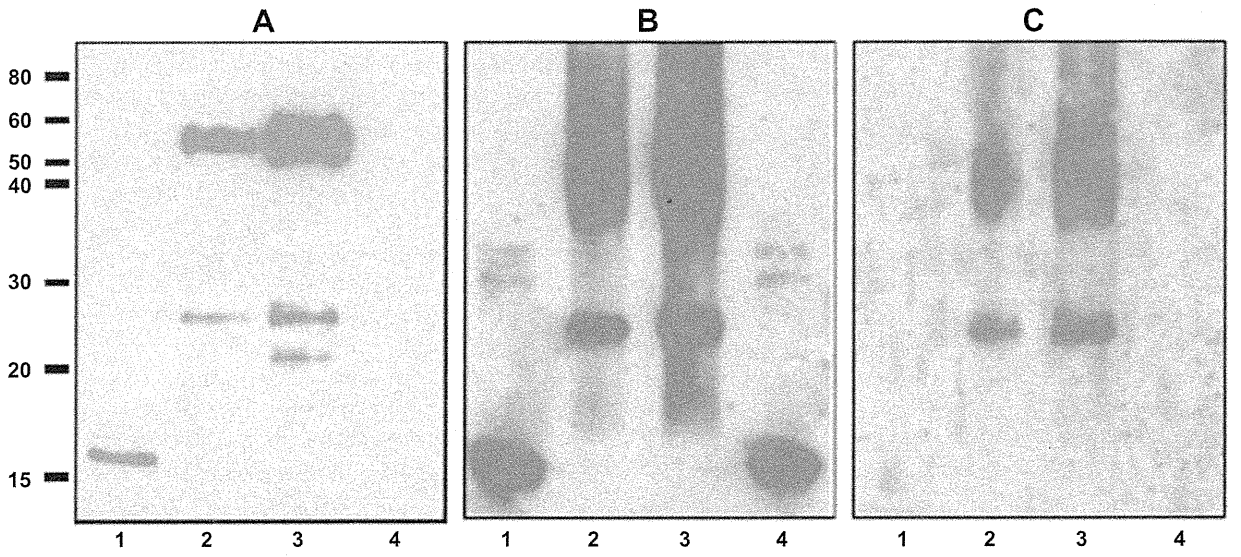

Figure 5. Immunoblot analysis of phosphorylated α-syn from plasma samples. Proteins immunocaptured from one plasma sample giving a low immunoassay signal for pS-α-syn protein (lane 2), and the other a high signal (lane 3), were immunoblotted along with recombinant phosphorylated α-syn (lane 1), and the recombinant nonphosphorylated standard (lane 4). *A*) Analysis with the phospho-dependent α-syn rabbit monoclonal antibody pS129 (Epitomics). *B*) Analysis with the rabbit polyclonal α-syn antibody FL-140 (Santa Cruz Biotechnology). Analysis with the rabbit polyclonal antiubiquitin antibody FL-76 (Santa Cruz Biotechnology).

protein. Nonetheless, the data can be compared within each individual immunoassay, although not necessarily across assays.

As far as we are aware, this is the first report to look at α-syn levels in repeat blood samples taken from individual patients with PD (collected here over an initial 3-mo period, from the first 32 patients enrolled into an ongoing longitudinal study) and also the first to detect phosphorylated forms of α-syn in blood plasma. One of the most important and novel results arising from this study is that although it is clear that the concentrations of α-syn vary greatly between individuals (for reasons that are, as yet, unknown), they remain remarkably consistent (at least over 3 mo) within the vast majority of individuals. This was a general finding for all four of the immunoassays. This lack of fluctuation of α-syn levels within individuals is a prerequisite for establishment of any viable biomarker. It has been reported that only a very small proportion of the α-syn in whole blood is present in peripheral blood mononuclear cells, platelets, and plasma, with the majority being present in red blood cells (46). Considering the abundance and fragility of red blood cells, α-syn levels in plasma, or other bodily fluids, such as CSF, could be artificially elevated in some samples by contamination with intact or lysed red blood cells (32). However, this type of contamination cannot be a confounding factor here, given the very high degree of consistency of α-syn concentrations within the plasma samples prepared from blood taken on 4 different occasions from the same individual. Moreover, it is unlikely that conditions, such as anemia would confound the results because all recruits with PD had undergone regularly blood screening for hemoglobin levels, and if anemia had been detected, it would have been treated.

The results of the 4 different immunoassays reveal that there was, statistically, no difference between the levels of total α-syn, oligo-α-syn, or oligo-pS-α-syn when comparing the 32 patients with PD with the healthy (nondiseased) control group of 30 individuals. This is not consistent with our previous findings for oligo-α-syn (37), which was elevated in PD. However, in our previous study, the control samples were obtained from individuals with serious medical conditions, such as stroke, heart disease, and cancer, and they were also taken at a different institution from the PD samples. In our current study, the controls were from healthy people, and variables such as the collection, separation and storage of the blood samples were more stringently controlled for. It should be noted that the oligo-α-syn immunoassay is the same as that reported in our previous publication (37), except for the detection system, which was changed from alkaline phosphatase (absorbance-based assay) to streptavidin-europium (time-resolved fluorescence). This has improved assay sensitivity and has allowed us to dilute the plasma samples to 1:25, whereas previously (37), the samples were not diluted. It is possible that this has also contributed to the different findings reported here. We now find that only the levels of pS-α-syn were higher in the PD group than in the control group (P=0.053), suggesting that the total phosphorylated protein may be the more useful diagnostic marker in plasma, and this is reflected in the ROC analysis for pS-α-syn (AUC=0.68). It should be noted that we did not make any formal adjustment for multiple testing (Bonferroni correction), because this is only a small-scale study, and this question will be addressed more fully in later work, when we have acquired and analyzed data from many more subjects.

The immunoblot results confirm that immunoreactive protein bands, with an intensity compatible with the immunoassay results, are detected when the protein from plasma is immunocaptured with N-19 and detected on immunoblots with pS129 (*i.e.*, the same capture and detection antibodies as those used for the pS-α-syn immunoassay). Some of these bands seem to represent ubiquitinated forms of the protein, since they also reacted with an antiubiquitin antibody. Whether these phosphorylated and ubiquitinated forms of α-syn originate from a cellular component in the blood itself or whether they originate from a peripheral tissue source elsewhere in the body, or from the brain (*via* CSF) is currently unknown.

Phosphorylation and ubiquitination are important secondary modifications of α-syn, with the protein deposited in LBs being predominantly phosphorylated at serine 129 (3, 47). Ubiquitination is a means of targeting a protein for destruction *via* the proteasome, and a defect in the ubiquitin-proteasome system is likely to be fundamental to the molecular pathogenesis of PD (48), although, recently, it has been suggested that α-syn phosphorylated at Ser-129 is targeted to the proteasome in a ubiquitin-independent manner (49). Phosphorylation of α-syn has been found to promote fibril formation, suggesting that hyperphosphorylation of α-syn might be a contributing factor in the pathogenesis of PD (47, 50). It has also been suggested that α-syn phophorylated at serine 129 and its aggregation are involved in pathway responsible for α-syn toxicity in oligodendrocytes (51, 52). Given this pathological role for phosphorylated and ubiquitinated forms of α-syn, the levels of these modified proteins in body fluids, including blood plasma, are more likely to reflect the fundamental neuropathology of PD than the normal protein (33). This inference is borne out by the results of the present study. Observations that 10–37% of aged, neurologically healthy controls display some α-syn pathology in their brains (53, 54), with about half of such subjects showing abundant α-syn pathology (53), could explain why the levels of pS-α-syn did not better discriminate between patients with PD and healthy controls.

It is also worth noting that the levels of the nonphosphorylated protein in plasma showed a weak but positive correlation with sampling age (of the patients with PD) in the present study, whereas the phosphorylated protein showed no such correlation. Age has already been noted as a confounding variable for total α-syn levels in CSF (32). This lack of correlation between

phosphorylated α-syn and age could be an additional advantage in its development as a potential molecular biomarker.

In summary, we have validated some novel assays for assessing α-syn levels in blood plasma; shown that these levels are highly consistent in repeat blood samples taken over 3 mo from patients with PD; presented evidence for the presence of pS-α-syn (phosphorylated at Ser-129) in blood plasma; and found that the mean level of pS-α-syn was marginally significantly higher (P=0.053) in the PD samples than in the controls. We accept that the latter result is preliminary and will need to be confirmed in larger-scale studies. Nevertheless, on the basis of the data presented here, further study of phosphorylated α-syn as a potential biomarker for PD and related α-synucleinopathies is clearly warranted. Moreover, whether any of the different forms of α-syn can be used to monitor the progression of PD cannot be determined from the present study with longitudinal sampling over 3 mo only and must await data from our ongoing longer-term longitudinal studies. FJ

The authors dedicate this paper to the memory of Prof. John Douglas Mitchell. The authors are grateful to the UK Medical Research Council for financial support (grant award G0601364). The authors thank all of the medical, nursing, and administrative staff of Dementias and Neurodegenerative Diseases Research Network North West, who assisted with the recruitment of patients and the collection and preparation of samples. We also wish to acknowledge and thank all the Consultant Neurologists and their staff within the North West Region of Great Britain who took part in this study, particularly Prof. J. Barrett (Arrowe Park Hospital, Wirral) and Drs. M. Kellett (Salford Royal Hospitals National Health Service Foundation Trust), S. N. H. Naqvi (Chorley and South Ribble District General Hospital), J. Raw (Fairfield General Hospital, Bury), M. J. Steiger (The Walton Centre, Liverpool), P. Tidswell (Royal Blackburn Hospital), C. J. Turnbull (Arrowe Park Hospital, Wirral), and J. Vassallo (Royal Oldham Hospital), for their enthusiasm for, and commitment to, the project. The authors thank students H. Sheldon, S. Macari, E. Mooney, and H. Kennedy from Lancaster Girls Grammar School for their help with the immunoblotting, and Mrs K. Lamb for her assistance in preparing the recombinant proteins.

REFERENCES

1. Spillantini, M. G., Schmidt, M. L., Lee, V. M., Trojanowski, J. Q., Jakes, R., and Goedert, M. (1997) α-Synuclein in Lewy bodies. *Nature* **388,** 839–840
2. Spillantini, M. G., Crowther, R. A., Jakes, R., Hasegawa, M., and Goedert, M. (1998) α-Synuclein in filamentous inclusions of Lewy bodies from Parkinson's disease and dementia with Lewy bodies. *Proc. Natl. Acad. Sci. U. S. A.* **95,** 6469–6473
3. Anderson, J. P., Walker, D. E., Goldstein, J. M., de Laat, R., Banducci, K., Caccavello, R. J., Barbour, R., Huang, J., Kling, K., Lee, M., Diep, L., Keim, P. S., Shen, X., Chataway, T., Schlossmacher, M. G., Seubert, P., Schenk, D., Sinha, S., Gai, W. P., and Chilcote, T. J. (2006) Phosphorylation of Ser-129 is the dominant pathological modification of α-synuclein in familial and sporadic Lewy body disease. *J. Biol. Chem.* **281,** 29739–29752
4. Chartier-Harlin, M. C., Kachergus, J., Roumier, C., Mouroux, V., Douay, X., Lincoln, S., Levecque, C., Larvor, L., Andrieux, J., Hulihan, M., Waucquier, N., Defebvre, L., Amouyel, P., Farrer, M., and Destee, A. (2004) α-Synuclein locus duplication as a cause of familial Parkinson's disease. *Lancet* **364,** 1167–1169
5. Ibáñez, P., Bonnet, A. M., Débarges, B., Lohmann, E., Tison, F., Pollak, P., Agid, Y., Dürr, A., and Brice, A. (2004) Causal relation between α-synuclein gene duplication and familial Parkinson's disease. *Lancet* **364,** 1169–1171
6. Singleton, A. B., Farrer, M., Johnson, J., Singleton, A., Hague, S., Kachergus, J., Hulihan, M., Peuralinna, T., Dutra, A., Nussbaum, R., Lincoln, S., Crawley, A., Hanson, M., Maraganore, D., Adler, C., Cookson, M. R., Muenter, M., Baptista, M., Miller, D., Blancato, J., Hardy, J., and Gwinn-Hardy, K. (2003) α-Synuclein locus triplication causes Parkinson's disease. *Science* **302,** 841
7. Polymeropoulos, M. H., Lavedan, C., Leroy, E., Ide, S. E., Dehejia, A., Dutra, A., Pike, B., Root, H., Rubenstein, J., Boyer, R., Stenroos, E. S., Chandrasekharappa, S., Athanassiadou, A., Papapetropoulos, T., Johnson, W. G., Lazzarini, A. M., Duvoisin, R. C., Di Iorio, G., Golbe, L. I., and Nussbaum, R. L. (1997) Mutation in the α-synuclein gene identified in families with Parkinson's disease. *Science* **276,** 2045–2047
8. Krüger, R., Kuhn, W., Müller, T., Woitalla, D., Graeber, M., Kösel, S., Przuntek, H., Epplen, J. T., Schöls, L., and Riess, O. (1998) Ala30Pro mutation in the gene encoding α-synuclein in Parkinson's disease. *Nat. Genet.* **18,** 106–108
9. Zarranz, J. J., Alegre, J., Gómez-Esteban, J. C., Lezcano, E., Ros, R., Ampuero, I., Vidal, L., Hoenicka, J., Rodriguez, O., Atarés, B., Llorens, V., Gomez Tortosa, E., del Ser, T., Muñoz, D. G., and de Yebenes, J. G. (2004) The new mutation, E46K, of α-synuclein causes Parkinson and Lewy body dementia. *Ann. Neurol.* **55,** 164–173
10. Volles, M. J., and Lansbury, P.T. Jr. (2003) Zeroing in on the pathogenic form of α-synuclein and its mechanism of neurotoxicity in Parkinson's disease. *Biochemistry* **42,** 7871–7878
11. Kayed, R., Head, E., Thompson, J. L., McIntire, T. M., Milton, S. C., Cotman, C. W., and Glabe, C. G. (2003) Common structure of soluble amyloid oligomers implies common mechanism of pathogenesis. *Science* **300,** 486–489
12. Masliah, E., Rockenstein, E., Veinbergs, I., Mallory, M., Hashimoto, M., Takeda, A., Sagara, Y., Sisk, A., and Mucke, L. (2000) Dopaminergic loss and inclusion body formation in α-synuclein mice: implications for neurodegenerative disorders. *Science* **287,** 1265–1269
13. Kahle, P. J., Neumann, M., Ozmen, L., Müller, V., Odoy, S., Okamoto, N., Jacobsen, H., Iwatsubo, T., Trojanowski, J. Q., Takahashi, H., Wakabayashi, K., Bogdanovic, N., Riederer, P., Kretzschmar, H. A., and Haass, C. (2001) Selective insolubility of α-synuclein in human Lewy body diseases is recapitulated in a transgenic mouse model. *Am. J. Pathol.* **159,** 2215–2225
14. Giasson, B. I., Duda, J. E., Quinn, S. M., Zhang, B., Trojanowski, J. Q., and Lee, V. M. (2002) Neuronal α-synucleinopathy with severe movement disorder in mice expressing A53T human α-synuclein. *Neuron* **34,** 521–533
15. Lo Bianco, C., Ridet, J. L., Schneider, B. L., Deglon, N., and Aebischer, P. (2002) α-Synucleinopathy and selective dopaminergic neuron loss in a rat lentiviral-based model of Parkinson's disease. *Proc. Natl. Acad. Sci. U. S. A.* **99,** 10813–10818
16. Irvine, G. B., El-Agnaf, O. M. A., Shankar, G. M., and Walsh, D. M. (2008) Protein aggregation in the brain: the molecular basis for Alzheimer's and Parkinson's diseases. *Mol. Med.* **14,** 451–464
17. Savitt, J. M., Dawson, V. L., and Dawson, T. M. (2006) Diagnosis and treatment of Parkinson disease: molecules to medicine. *J. Clin. Invest.* **116,** 1744–1754
18. Suchowersky, O., Reich, S., Perlmutter, J., Zesiewicz, T., Gronseth, G., and Weiner, W. J. (2006) Practice parameter: diagnosis and prognosis of new onset Parkinson disease (an evidence-based review): report of the Quality Standards Subcommittee of the American Academy of Neurology. *Neurology* **66,** 968–975
19. Hughes, A. J., Daniel, S. E., Kilford, L., and Lees, A. J. (1992) Accuracy of clinical diagnosis of idiopathic Parkinson's disease: a clinico-pathological study of 100 cases. *J. Neurol. Neurosurg. Psychiatry* **55,** 181–184
20. Hughes, A. J., Daniel, S. E., and Lees, A. J. (2001) Improved accuracy of clinical diagnosis of Lewy body Parkinson's disease. *Neurology* **57,** 1497–1499
21. Schapira, A. H. V. (1999) Science, medicine, and the future: Parkinson's disease. *Brit. Med. J.* **318,** 311–314